AFRL-AFOSR-VA-TR-2019-0320

Phase-Controlled Magnetron Development

Jim Browning
BOISE STATE UNIVERSITY

05/21/2019
Final Report

DISTRIBUTION A: Distribution approved for public release.

Air Force Research Laboratory
AF Office Of Scientific Research (AFOSR)/ RTB1
Arlington, Virginia 22203
Air Force Materiel Command

REPORT DOCUMENTATION PAGE

Form Approved
OMB No. 0704-0188

1. REPORT DATE *(DD-MM-YYYY)*
05/15/2019

2. REPORT TYPE
Final

3. DATES COVERED *(From - To)*
15 Feb 2016 to 14 Feb 2019

4. TITLE AND SUBTITLE
Phase-Controlled Magnetron Development

5a. CONTRACT NUMBER
FA9550-16-1-0083

5b. GRANT NUMBER

5c. PROGRAM ELEMENT NUMBER

6. AUTHOR(S)
Jim Browning, Andy Yue, and Don Plumlee, Boise State University
Tayo Akinwande and Winston Chern, Massachusetts Institute of Technology

5d. PROJECT NUMBER

5e. TASK NUMBER

5f. WORK UNIT NUMBER

7. PERFORMING ORGANIZATION NAME(S) AND ADDRESS(ES)
Boise State University
1910 University Dr.
Boise, ID 83725-0001

8. PERFORMING ORGANIZATION REPORT NUMBER

9. SPONSORING/MONITORING AGENCY NAME(S) AND ADDRESS(ES)
Air Force Office of Scientific Research
875 North Randolph Street, Rm3113
Arlington, VA 22203-1954

10. SPONSOR/MONITOR'S ACRONYM(S)
AFOSR

11. SPONSOR/MONITOR'S REPORT NUMBER(S)

12. DISTRIBUTION/AVAILABILITY STATEMENT
Distribution A

13. SUPPLEMENTARY NOTES

14. ABSTRACT
This project involved the development of a cathode structure using Gated Field Emission Arrays (GFEAs) that could be modulated at the operating frequency of a magnetron to control electron injection. The goal was to inject the electrons to preferentially form the electron spokes in a 75 kW industrial cooker magnetron. An experiment was developed using the L3 Technologies CWM75KW which can operate as low as 1 kW with an injection current of 150 mA and at a frequency of 915 MHz. The experiment replaced the helical cathode in the magnetron with a ceramic based structure that used integrated interconnects, vias, and traces to support 30 GFEA die in a 10-sided configuration. Facet plates are placed over the die to p

15. SUBJECT TERMS

16. SECURITY CLASSIFICATION OF: a. REPORT	b. ABSTRACT	c. THIS PAGE	17. LIMITATION OF ABSTRACT	18. NUMBER OF PAGES	19a. NAME OF RESPONSIBLE PERSON
					Jim Browning
					19b. TELEPHONE NUMBER *(Include area code)*
U	U		UU	30	208-426-2347

Standard Form 298 (Rev. 8/98)
Prescribed by ANSI Std. Z39.18

INSTRUCTIONS FOR COMPLETING SF 298

1. REPORT DATE. Full publication date, including day, month, if available. Must cite at least the year and be Year 2000 compliant, e.g. 30-06-1998; xx-06-1998; xx-xx-1998.

2. REPORT TYPE. State the type of report, such as final, technical, interim, memorandum, master's thesis, progress, quarterly, research, special, group study, etc.

3. DATE COVERED. Indicate the time during which the work was performed and the report was written, e.g., Jun 1997 - Jun 1998; 1-10 Jun 1996; May - Nov 1998; Nov 1998.

4. TITLE. Enter title and subtitle with volume number and part number, if applicable. On classified documents, enter the title classification in parentheses.

5a. CONTRACT NUMBER. Enter all contract numbers as they appear in the report, e.g. F33315-86-C-5169.

5b. GRANT NUMBER. Enter all grant numbers as they appear in the report. e.g. AFOSR-82-1234.

5c. PROGRAM ELEMENT NUMBER. Enter all program element numbers as they appear in the report, e.g. 61101A.

5e. TASK NUMBER. Enter all task numbers as they appear in the report, e.g. 05; RF0330201; T4112.

5f. WORK UNIT NUMBER. Enter all work unit numbers as they appear in the report, e.g. 001; AFAPL30480105.

6. AUTHOR(S). Enter name(s) of person(s) responsible for writing the report, performing the research, or credited with the content of the report. The form of entry is the last name, first name, middle initial, and additional qualifiers separated by commas, e.g. Smith, Richard, J, Jr.

7. PERFORMING ORGANIZATION NAME(S) AND ADDRESS(ES). Self-explanatory.

8. PERFORMING ORGANIZATION REPORT NUMBER. Enter all unique alphanumeric report numbers assigned by the performing organization, e.g. BRL-1234; AFWL-TR-85-4017-Vol-21-PT-2.

9. SPONSORING/MONITORING AGENCY NAME(S) AND ADDRESS(ES). Enter the name and address of the organization(s) financially responsible for and monitoring the work.

10. SPONSOR/MONITOR'S ACRONYM(S). Enter, if available, e.g. BRL, ARDEC, NADC.

11. SPONSOR/MONITOR'S REPORT NUMBER(S). Enter report number as assigned by the sponsoring/ monitoring agency, if available, e.g. BRL-TR-829; -215.

12. DISTRIBUTION/AVAILABILITY STATEMENT. Use agency-mandated availability statements to indicate the public availability or distribution limitations of the report. If additional limitations/ restrictions or special markings are indicated, follow agency authorization procedures, e.g. RD/FRD, PROPIN, ITAR, etc. Include copyright information.

13. SUPPLEMENTARY NOTES. Enter information not included elsewhere such as: prepared in cooperation with; translation of; report supersedes; old edition number, etc.

14. ABSTRACT. A brief (approximately 200 words) factual summary of the most significant information.

15. SUBJECT TERMS. Key words or phrases identifying major concepts in the report.

16. SECURITY CLASSIFICATION. Enter security classification in accordance with security classification regulations, e.g. U, C, S, etc. If this form contains classified information, stamp classification level on the top and bottom of this page.

17. LIMITATION OF ABSTRACT. This block must be completed to assign a distribution limitation to the abstract. Enter UU (Unclassified Unlimited) or SAR (Same as Report). An entry in this block is necessary if the abstract is to be limited.

Phase-Controlled Magnetron Development

Final Report

May 15, 2019

FA#9550-16-1-0083

Jim Browning, Andy Yue, and Don Plumlee, Boise State University

Tayo Akinwande and Winston Chern, Massachusetts Institute of Technology

ABSTRACT

This project involved the development of a cathode structure using Gated Field Emission Arrays (GFEAs) that could be modulated at the operating frequency of a magnetron to control electron injection. The goal was to inject the electrons to preferentially form the electron spokes in a 75 kW industrial cooker magnetron. An experiment was developed using the L3 Technologies CWM75KW which can operate as low as 1 kW with an injection current of 150 mA and at a frequency of 915 MHz. The experiment replaced the helical cathode in the magnetron with a ceramic based structure that used integrated interconnects, vias, and traces to support 30 GFEA die in a 10-sided configuration. Facet plates are placed over the die to protect them from the interaction space, and each plate had 2 slits which act as electron hop funnels. The entire cathode structure and GFEA test and integration process was completed. GFEA die were specifically designed for implementation into the cathode structure. Each GFEA die was required to generate 5-7 mA to drive the magnetron; however only 2 mA was achieved for these large die because of shorting and leakage currents. Simulation efforts included a model of the magnetron using both a simple cylindrical cathode and a 10-sided cathode to match the experiment. Simulations at the typical magnetron parameters (5 A, -17 kV, and 1800 G) only demonstrated oscillation if cavity RF priming was used for as little as 20 ns with oscillation beginning at 100 ns. The modulated cathode concept was also studied with electron injection at the operating frequency to control spoke formation, and that model also showed oscillation after 120 ns.

I. Introduction

This research project uses both experiment and simulation to study and to demonstrate the phase control of a commercial magnetron. The magnetron is the CWM-75KW from L-3 Communications. In our approach, Gated Field Emission Arrays (GFEAs) are used as the cathode and are modulated at the magnetron operating frequency so that electrons can be injected at the desired spatial location and time to form the electron spokes. Prior simulation work using the code VSim has shown that this electron injection can dynamically control the magnetron phase. This report provides the results from the three year program of research which includes implementation of our magnetron driver and our GFEA test system, completion of our magnetron cathode mechanical structure, simulation of the cathode delay/transmission line, and simulation of the L3 magnetron using VSIM.

II. Magnetron Experimental System Approach

In our approach we worked closely with L-3 EDD Communications in Williamsport, PA. L3 has provided our group with their entire assembly for the CWM-75KW commercial magnetron. The magnetron is a 10 cavity cooker magnetron that normally operates at up to 75 kW CW at a frequency from 900-915 MHz. Table 1 provides the typical operating parameters for the magnetron including HV, current, and magnetic field. Although the injection current is high (5 A), L-3 was able to operate the magnetron at much low current (150 mA) and power (<1 kW) making it much easier to implement a GFEA cathode. Based on this result, it was clear that the L-3 magnetron was a good fit for our approach. The experimental operating parameters are also given in Table 1, and it is clear that in addition to the lower required current, the required high voltage drops from -17 kV to -8.3 kV. These lower values make the modulated cathode experiment easier to implement. However, the vacuum test chamber system was not designed to work with the L-3 magnetron, and the cathode used in the L-3 magnetron is only 1.47 cm in diameter. This smaller diameter makes cathode fabrication more difficult and makes the GFEA die smaller than originally planned.

Table 1. L-3 Commercial magnetron typical and experimental operating parameters

Magnetron	**Cathode Voltage**	**Injection Current**	**Magnetic Field**	**Frequency**
Typical CWM-75KW	-17 kV	5 A	1700 G	915 MHZ
Experiment based on L3 Data	- 8.3 kV	150 mA	900 G	907 MHz

The 10-sided faceted cathode for the experiment has been designed to fit within the L-3 magnetron assembly. This cathode design is described in detail later. Shown in Fig. 1 is the drawing of the L-3 magnetron with the faceted cathode in place along with an expanded view so that the cathode is more clearly visible. The vacuum test chamber system was reconfigured to allow for the new magnetron approach. L-3 welded a 6" conflat flange onto their magnetron assembly and provided BSU with the assembly, the electromagnet, the coupling waveguide, the directional coupler, and the dummy load. Shown in Fig. 2 is the actual vacuum test chamber along with the magnetron cavity attached to the chamber. At the top of the magnetron cavity is the coupling antenna which is inserted into the coupling waveguide. The vacuum system is pumped using a roughing pump and a turbomolecular pump. The cathode is placed inside the lower vacuum chamber for insertion up into the magnetron cavity. The alignment/support structure was completed. The L-3 magnetron coupling waveguide and magnets were attached to the chamber as shown in Fig. 3. This part of the system is complete.

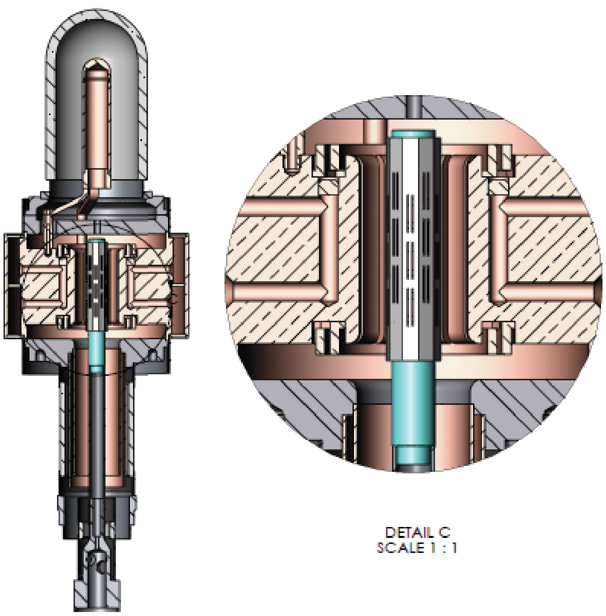

Figure 1. L-3 magnetron assembly with BSU cathode design

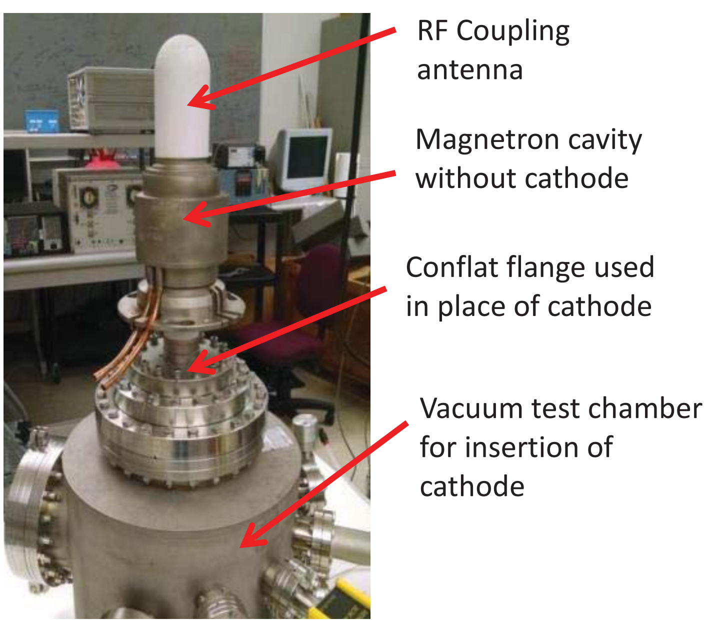

Figure 2. Vacuum test chamber assembly with L-3 magnetron in place using 6" conflat flange.

Figure 3. Photograph of chamber system with electromagnets and coupling waveguide in place.

III. Cathode Structure Design and Fabrication

The major design and fabrication efforts over the last 3 years has been in the 10-sided faceted cathode. This structure is fabricated from a Low Temperature Co-Fired Ceramic (LTCC) and acts as both a mechanical and electrical system. The structure supports, protects, and connects the GFEA die used for the controlled electron injection. After a major design and fabrication effort, a design was finalized, and this design and its fabrication are described here. As the magnetron is a 10-cavity device, it is necessary to drive 5 electron spokes in phase. The cathode structure is divided azimuthally into 10 facet plates.

Each plate contains 2 hop funnel slits for electron injection. Therefore, each electron spoke is divided into 4 phase elements, each 90° apart. With 2 phase elements per facet plate (one for each slit), there are then 20 controllable elements azimuthally around the cathode. This structure is shown in Fig. 4. Note that in addition to the 2 slits per facet azimuthally, there are 3 sets of slits placed axially for each facet. These slits are for 3 different die placed axially. Each GFEA die is divided into 2 phase elements by using different gate connections. The 3 die are placed axially so that each die is not too long because of RF attenuation or too difficult to fabricate. As described later, each die is 7 mm x 2.5 mm. Therefore, for modulation of the electron injection, electrons must be injected through 5 sets of axial slits at 5 different azimuthal locations. To generate the

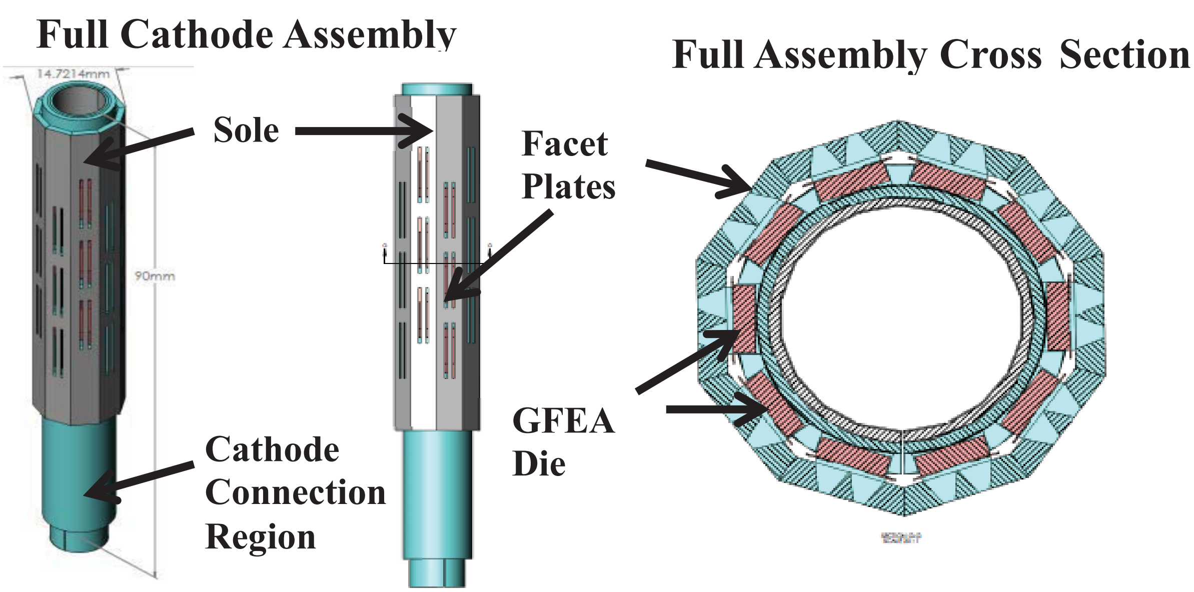

Figure 4. Cathode structure assembly showing a 10-sided cathode consisting of 10 facet plates, each with 2 slits azimuthally and 3 sets of slits axially per facet plate. GFEA die are beneath the facet plates. A cross section view shows the hop funnel facet plates, the GFEA die, and the internal structure.

phase separation for 4 phase elements to control 5 electron spokes, the cathode structure is fabricated as a delay line.

With 5 spokes that must be driven with 4 phase elements, it is necessary to split the drive lines into 5 traces. Each trace is designed as a 50 Ω micro-strip line with upper and lower ground planes. Therefore, each of the 5 traces is placed between 2 ground planes, and electrical vias must be used to connect the trace to the GFEA die gates by passing through the upper (radially) ground plane. An exploded view of this structure is shown in Fig. 5. As can be seen in the exploded view, the facet plates cover the GFEA die to protect the die from the interaction space. These plates contain slits (hop funnels) so that the electrons can be injected into the interaction space. Under each facet plate are 3 die spaced axially. Each die is divided into 2 phase elements, and the gates are connected by electrical jumpers. These jumpers (silver paste) connect the through-hole vias in the LTCC to the die gates. The vias go through the outer ground plane to the transmission lines. The outer ground plane also is used to connect the back side of the GFEA die. Therefore, the emitter tips are

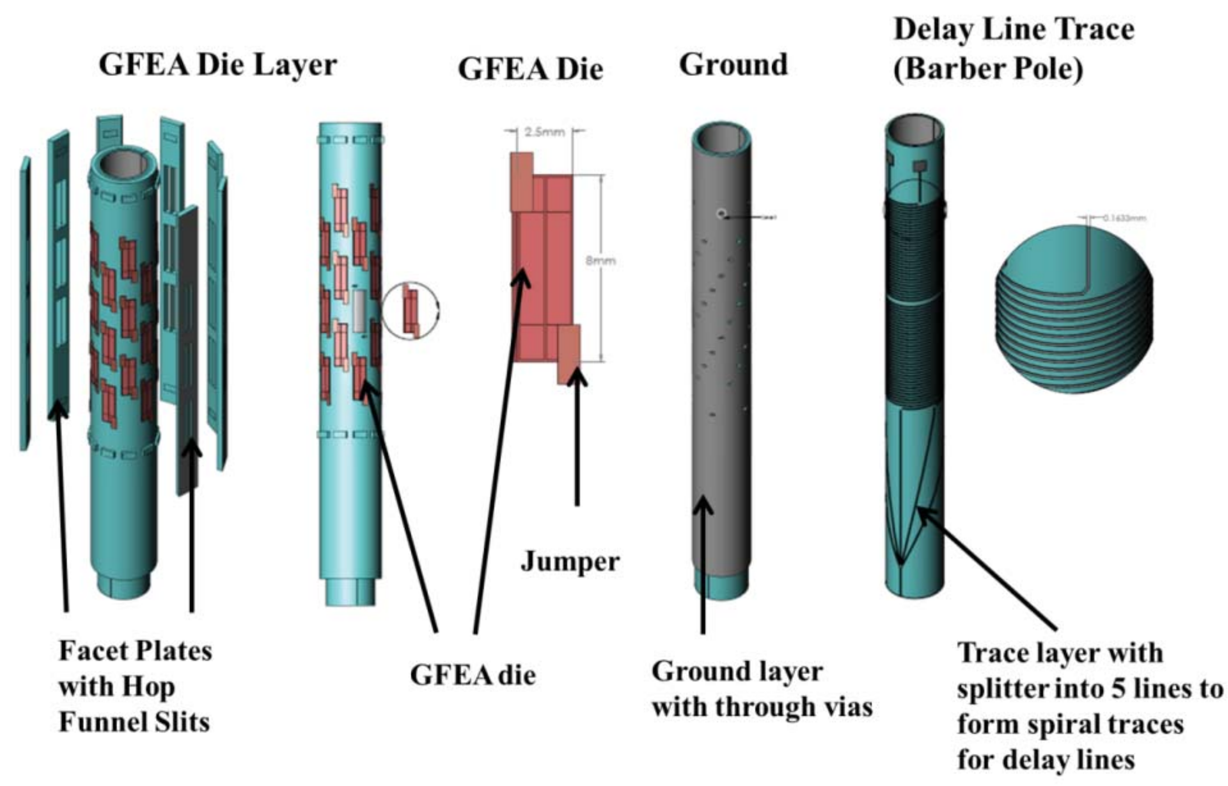

Figure 5. Layout and assembly drawing of the cathode structure fabricated in LTCC. On the left is an exploded view showing the facet plates and the GFEA die beneath. Each GFEA die is divided azimuthally into 2 addressable elements. Three die are placed axially beneath each facet plate. Electrical interconnects (jumpers) connect the transmission line via sot the GFEA gates. The single RF signal is split into 5 transmission line traces which spiral upward in a barber pole configuration. The die vias are staggered as are the die so that a 90° delay can be achieved.

connected to the local ground plane, and the gates are modulated. To achieve the 90° phase delay for the 4 phase elements, the RF input signal is divided into 5 traces. As each of these traces travels around the cathode in a helix (barber pole) and moves axially up, a 90° phase delay occurs approximately every rotation. Each via is placed at the exact location that provided the desired phase separation. Hence, one RF input signal can be used to drive all of the GFEA die. The delay lines are designed so that the 4 phase elements can be achieved at the 5 spoke locations.

We have completed design and fabrication of this structure with the exception of the delay line, which is still being designed and simulated. The fabrication process is not described here; however this structure is new in the use of LTCC and is expected to be of interest to engineers building cylindrical RF structures such as meta-materials. The entire structure is fabricated in layers in the LTCC green state. The metal traces (Ag) are printed using a screen printer. The vias are machined using a laser mill. After all of the layers are fabricated in the green state, they are assembled on a jig and laminated in a hydrostatic press. Then the entire assembly is fired at 800C to its final state. About a 15% shrinkage occurs, so the design must compensate for the shrinkage. Shown in Fig. 6 are photographs of the LTCC layers before they are rolled into the cylindrical structure. Here the vias and slots for the GFEA die are clearly visible.

These efforts required numerous iterations and process studies. A thorough study of various alignment, lamination, and firing techniques were studied. The resulting study [1] resulted in the final process flow that is now used in the project. Shown in Fig. 7 are some examples of the LTCC structure with dummy die and facet plates. Also, an example of how the device would look in the L-3 magnetron is shown. Note that the cathode structure will actually be longer to accommodate mounting in the chamber, to accommodate the trace split, to mount end hats, and to attach to the support stand.

The entire device structure on the support stand is shown in Fig. 7. This structure has been assembled and placed in the vacuum test chamber with all electrical connections, so this part of the system is complete.

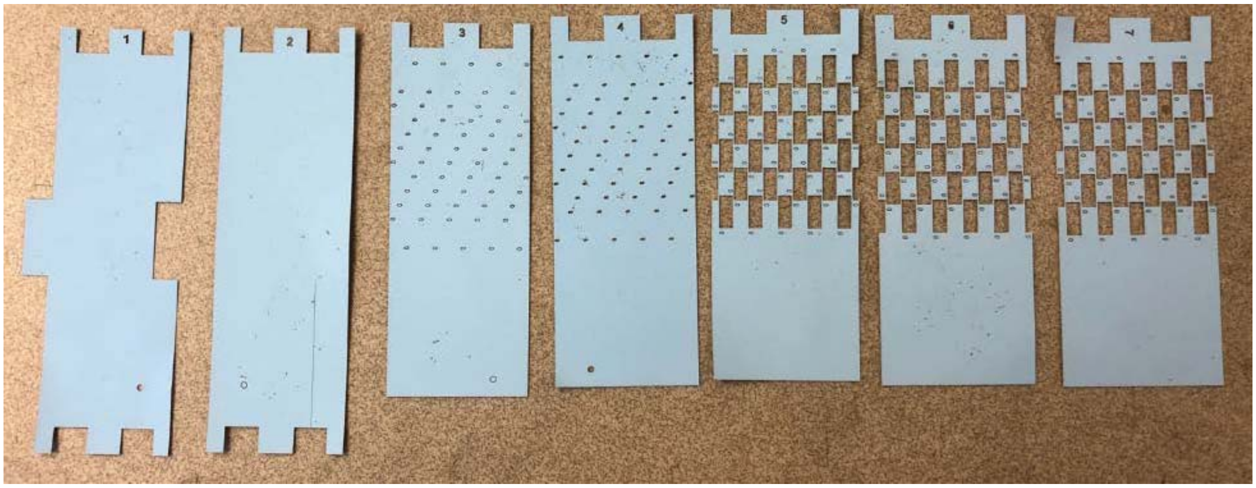

Figure 6. Photographs of the LTCC layers before being rolled into the cylindrical structure. Metal traces are not shown here, but the vias and slots for the GFEA die are clearly seen on the right side images.

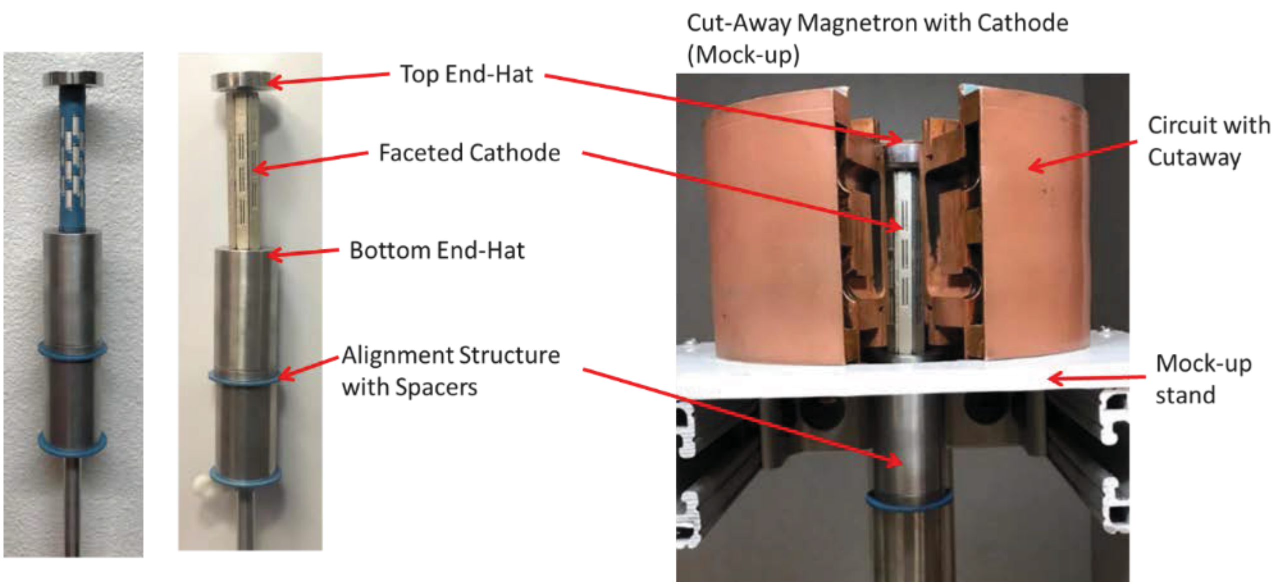

Figure 7. Photographs of the cathode support stand showing the alignment structure and end-hats with the LTCC structure without die (left), the full structure with facet plates (center), and the proof-of-concept in a magnetron circuit cut-away (right).

IV. Cathode Driver System

For this project there are 2 driver systems. The first system is used to drive a 10 µs pulse to generate current from all of the emitters simultaneously. This system is the Continuous Current driver. The second system is intended to drive an RF signal on the cathode transmission delay line as described above. This system is the Modulated Current driver. These systems are described in more detail below. Both of these systems use a wireless communication setup between a National Instruments LabView control system and the high voltage floating deck. This setup is also described.

A. Control System and Floating Deck

The cathode driver system must float at the cathode potential of -8.3 kV. In addition to the drivers, several power supplies are also required. A Glassman HV power supply floats the entire deck and can drive 200 mA. As the current flows through the emitter tips, the emission current flows through the HV power supply through the cathode structure transmission line ground plane. Hence, the emission current is not through the emitter gates which should have low leakage current. A picture of the completed system is shown in Fig. 9.

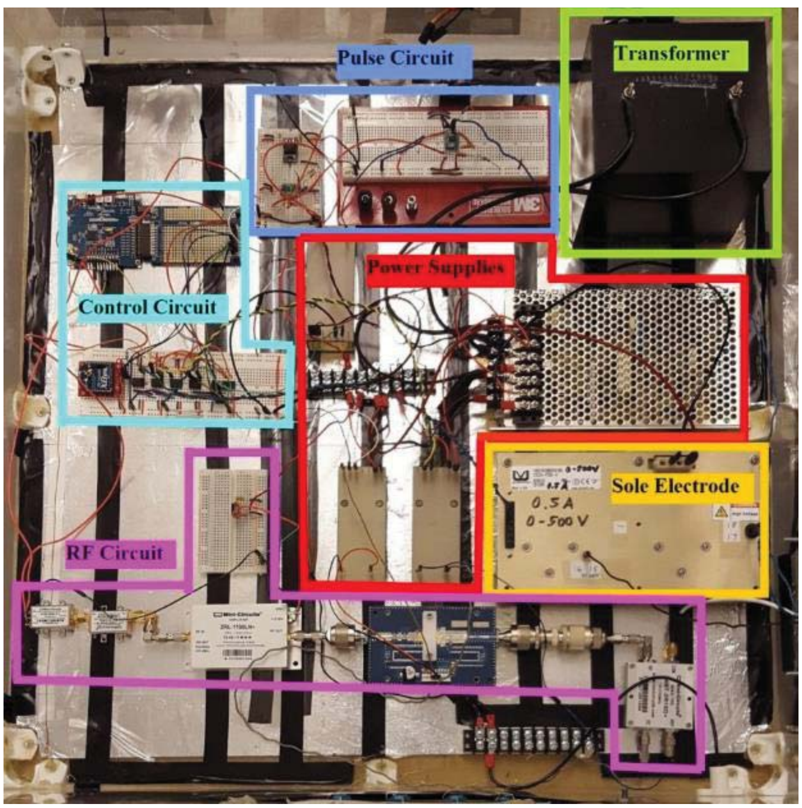

Figure 9. Photograph of the HV control platform with wireless communication.

A ZigBee wireless system provides the communication between the National Instruments LabView control hardware and software and the floating deck. An Atmel Microcontroller receives commands from the system and initiates either test measurements or the 10 us emission pulse. An isolation transformer provides the AC power to all of the DC hardware. Depending upon the driver configuration, DC to DC converters are used to power the sole electrode bias, the OP-AMP or Bias Tee voltage, and the RF amplifier (MOSFET). These are described below. The Atmel microcontroller sends signals to all of the system components to set bias voltages, set timing and frequencies, and to initiate the experimental pulse. The output of the magnetron and other systems are monitored both at HV and at ground. Most measurements of the pulse are at ground potential for the National Instruments hardware and for our high frequency oscilloscope.

These diagnostics include the output power directional coupler and three current transformers. During a pulse, the magnetron output is directed to a dummy load. The output from a waveguide directional coupler is sent to a 4GHz, 4 channel oscilloscope. Therefore, we can directly measure the RF output signal and store these measurements to determine power and phase. One current transformer is used to measure the current through the Glassman HV power supply. This current will include the injected electron current into the magnetron and any leakage or displacement current. A second current transformer is used to measure the sole electrode current. This current includes injection current that returns to the sole (back bombards) as well as any leakage current. Finally, a third transformer measures the current on the GFEA gate. For the Continuous current system, this current will measure the leakage current of the gate as well as any displacement current. For the Modulated Driver, this measurement will also monitor the RF modulated current. Finally, of the relevant voltages and currents including the HV bias, magnet current, sole bias, and gate bias are also measured. A pictorial representation is shown in Fig. 10.

As shown in Fig. 10, the HV power supply floats the entire system. The pictorial shows the GFEAs as a substrate with a ground plane, tips, and field emitter gates. The local ground plane of the

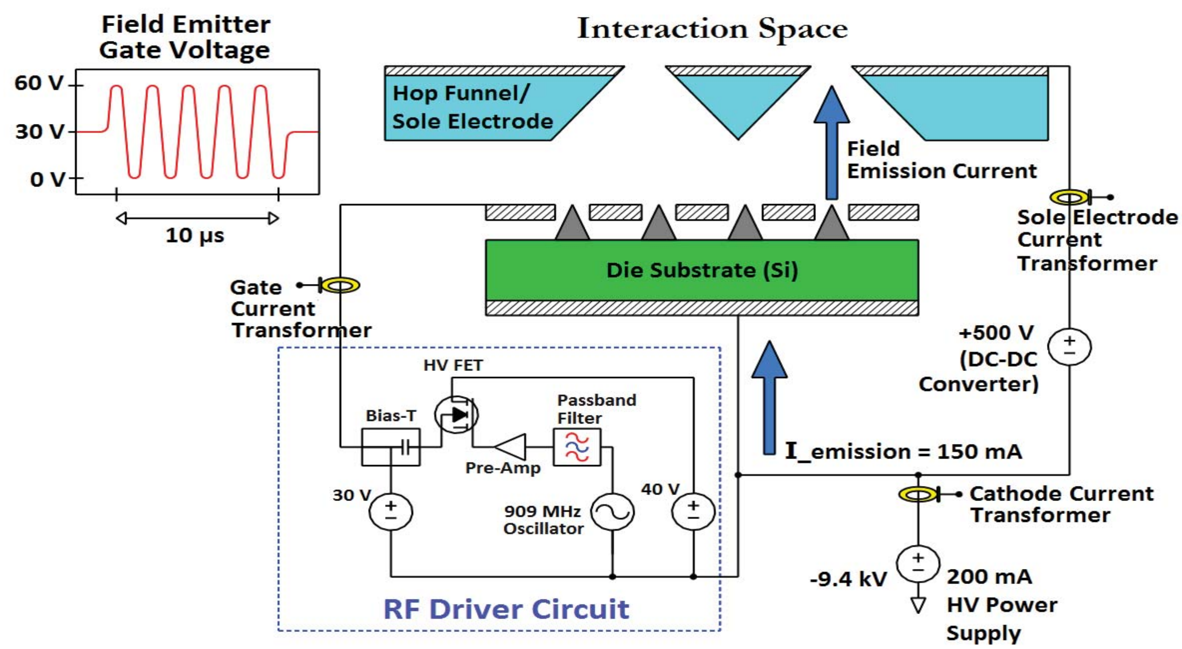

Figure 10. Driver pictorial system showing the Continuous Current driver scheme. Current transformers measure the gate current, sole electrode current, and emission current. A HV Op-AMP is used to provide the gate pulse using a DC offset. DC-DC converters provide the hop/sole bias relative to the HV power supply. Emission current flows through the GFEA die backside as part of the transmission line local ground.

substrate is connected to the ground of our LTCC cathode structure which is at -9.4 kV. The Field Emitter Gate Voltage pulse is relative to this local ground. Emission current flows through the ground plane, the silicon substrate, and the emitter tips and into the electron hop funnels. As shown, the hop funnel electrode is also the sole electrode which sets the electric field in the magnetron interaction space. Electrons are accelerated out of the hop funnel slits by the 500 V difference between the GFEA die and the sole electrode bias. Via secondary emission, the electrons "hop" out through the hop funnel slits.

B. Continuous Current Driver

This driver system must bias the GFEA gates in the 50 to 70 V range depending upon the required injection current and the quality of the GFEAs. For continuous current, a slow rise and fall 10 us pulse is needed. However, because the GFEAs have a "turn on" current, it is not necessary to drive the bias voltage from 0 to 70 V. This important aspect is described in more detail later. For the continuous current driver, a HV OP-AMP capable of 100 V is used to drive the gate pulse as shown in Fig. 8. A battery is used to create a small DC offset in the OP-AMP input. A pulse generator is used to create the 10 us pulse input (not shown). The combined offset and pulse can then create a total voltage pulse ranging from a continuous 30 V to a peak 60V. This system is complete.

C. Modulated Current DriverThe modulated driver system is similar in concept to the Continuous Current Driver. The pictorial representation of Fig. 10 can be used as a reference. The major difference is that the OP-AMP and pulse generator must be replaced with an RF amplifier chain to generate the 15 to 20 V RF signal to drive the GFEA gates. As shown in the pictorial in Fig. 11 (top), a voltage controlled oscillator (VCO) is used to generate the modulation signal from 905-910 MHz. This output is driven through a bandpass filter, a phase shifter, and a pre-amplifier. The 26 dBm output then drives a Cree HV MOSFET board to achieve around 36 dBm. This board will be tuned in the future to get a higher power. The RF signal is then run through a Bias Tee (not shown in schematic) to add a DC offset of 30-40 V. Therefore, the RF signal (eventually 20-25V) is driven on top of the DC signal to modulate the gates at the RF frequency. As shown in Fig. 11 (bottom), this driver system has already been assembled and tested, and the results show that we can drive the system as desired.

D. GFEA Sinusoidal Drive Scheme

Originally, the concept was to use different phase control circuits to control each phase, but this idea was abandoned for the phase delay transmission line approach for simplicity. In addition, although the original idea was to use a pulse, it was clear that a sinusoidal RF signal is a much better method for driving the GFEA gates as it is easier to design a transmission line, pulse related frequency components are removed, and RF amplifiers are easier to obtain. In addition, because we want to use a DC offset to minimize the required modulation voltage, a sinusoid provides a much cleaner On/OFF drive. This work is complete except for the delay transmission line modeling and test.

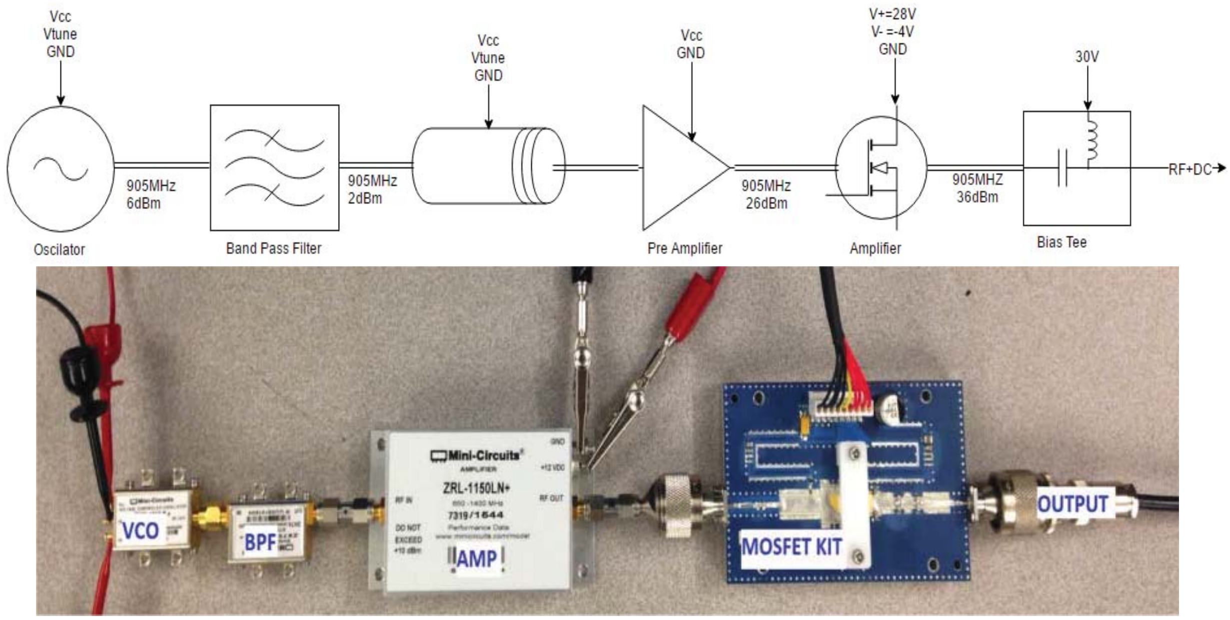

Figure 11. Modulated Current Driver system (top) schematic and (bottom) prototype hardware. A voltage controlled oscillator provide the RF drive signal. A small signal amplifier is used to drive a medium voltage (20V) MOSFET. The RF output is driven through a Bias Tee to provide a DC offset for the GFEA gate bias.

V. Delay Line Simulation and Experiments

In order for the delay line concept to work, the transmission line must be designed to split into 5 traces and impedance matched as a resonant circuit to the 30 GFEA die on the cathode structure. In principle, each GFEA die is a capacitor with some leakage current (high resistance). So the simulation efforts have looked at a stripline with capacitors attached to determine if the reactive load can be matched. To terminate the line, a 50 Ω resistor is needed at the end of the circuit. There is no physical room to connect another transmission line at the top of the cathode to connect to an external resistor. We have developed a resistor internally using the DuPont resistor past material. However, the results have been inconsistent with it difficult to consistently achieve 50 Ω. More process development is required.

Simulation of the transmission line has been performed using the simulations COMSOL and CST Studio. Based on the results, we have chosen to switch entirely to CST for our future modelling efforts. Shown in Fig. 12 are the drawing of the transmission line used in the modelling (top left) and the COMSOL simulation model (top right). To test the model, a simple flat transmission line has been fabricated using LTCC. An example of this is shown in Fig. 12 (bottom). The photograph shows the SMA connectors and the location of the slot where the GFEA die is place. Experimentally the impedance of the structure is measured with a network analyzer and was found close to 50 Ω. In more recent experiments with actual GFEA die, the impedance was, of course, off, so the CST modeling is looking at impedance matching with an actual GFEA die using the measured die capacitance.

This work was extended to the CST simulation. As shown in Fig. 13, the CST model is used (upper left) with an equivalent die capacitance. A matching circuit (upper right) is modeled to impedance match the GFEA die on the transmission line. This matching circuit greatly improves the impedance match to 50 Ω as seen in both the lower left and lower right images of the Smith chart where the Red symbol is the matched circuit.

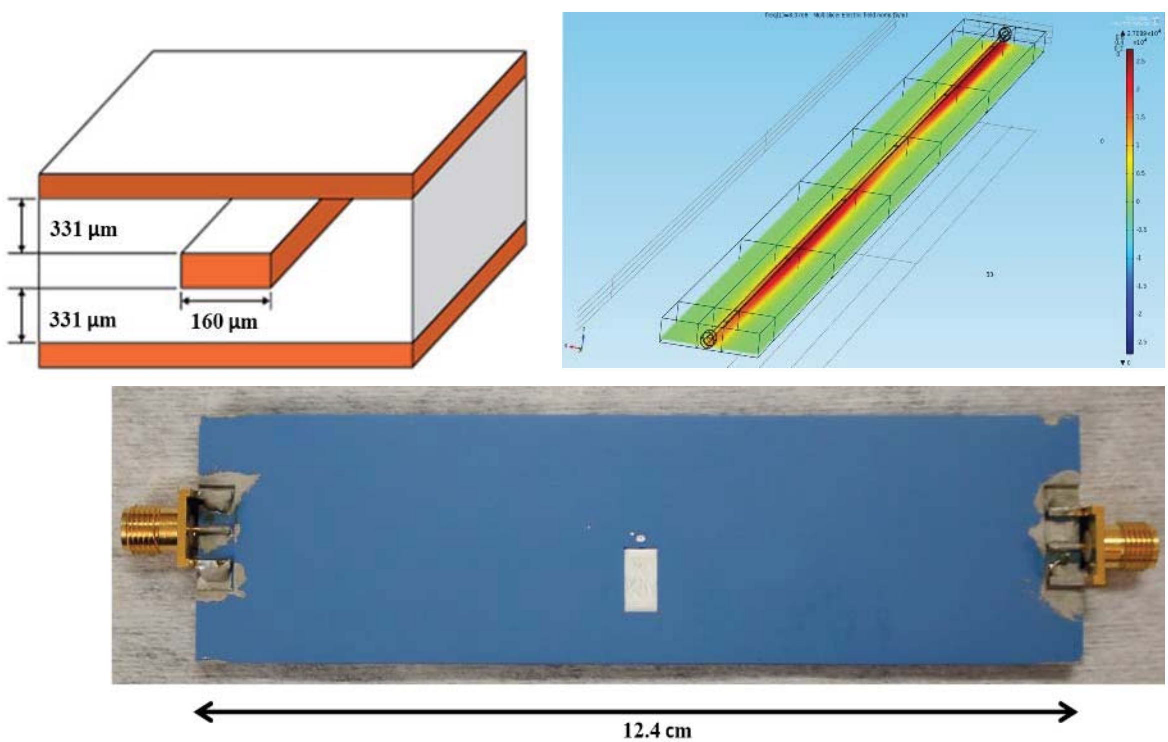

Figure 12. (Top left) Drawing of the 50Ω transmission line design used for the cathode structure , ((top right) COMSOL model of the transmission line, and (bottom) picture of a transmission line test structure fabricated in LTCC with a GFEA die location.

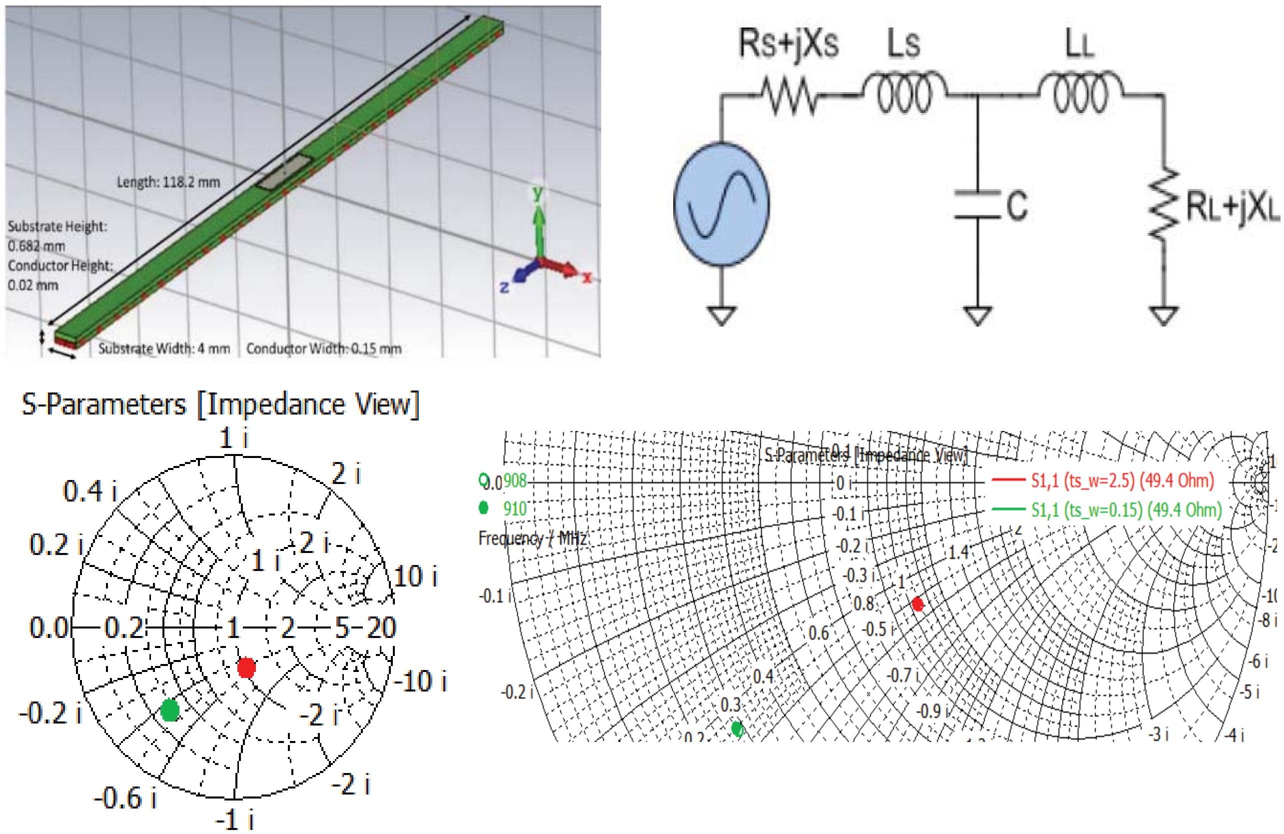

Figure 13. CST simulations of the stripline with (upper left) the CST model, (upper right) the matching circuit, (lower left) the Smith chart predictions from the simulation, and (lower right) the magnified Smith chart. Red is matched and green is not matched.

VI. GFEA Die Design and Fabrication

A. Design

The GFEAs for the cathode structure must be designed and fabricated to allow for assembly onto the structure and easy interconnection. The die geometry was determined by the cathode diameter and the hop funnel facet plate size. In addition, the process flow for fabrication uses a stepper window that needed to match the appropriate geometry for the cathode leaving enough space for interconnects. Because some die on the cathode are connected from the top and some from the bottom, it was determined that it was most appropriate to make an entirely symmetric die. The die must also be divided into 2 section (phase elements), so there is a gap in the gate metal. The layout of the die structure is shown in Fig. 14 along with an image of a fully fabricated die. The large gate metal sections on the top and bottom are for the interconnect jumpers. This layout is designed to fit in the stepper window size. With 3 die per facet, we need 30 die for a cathode. With an injection current of 150 mA needed for magnetron oscillation, this die design results in a 5 mA/die requirement or ~200 mA/cm^2.

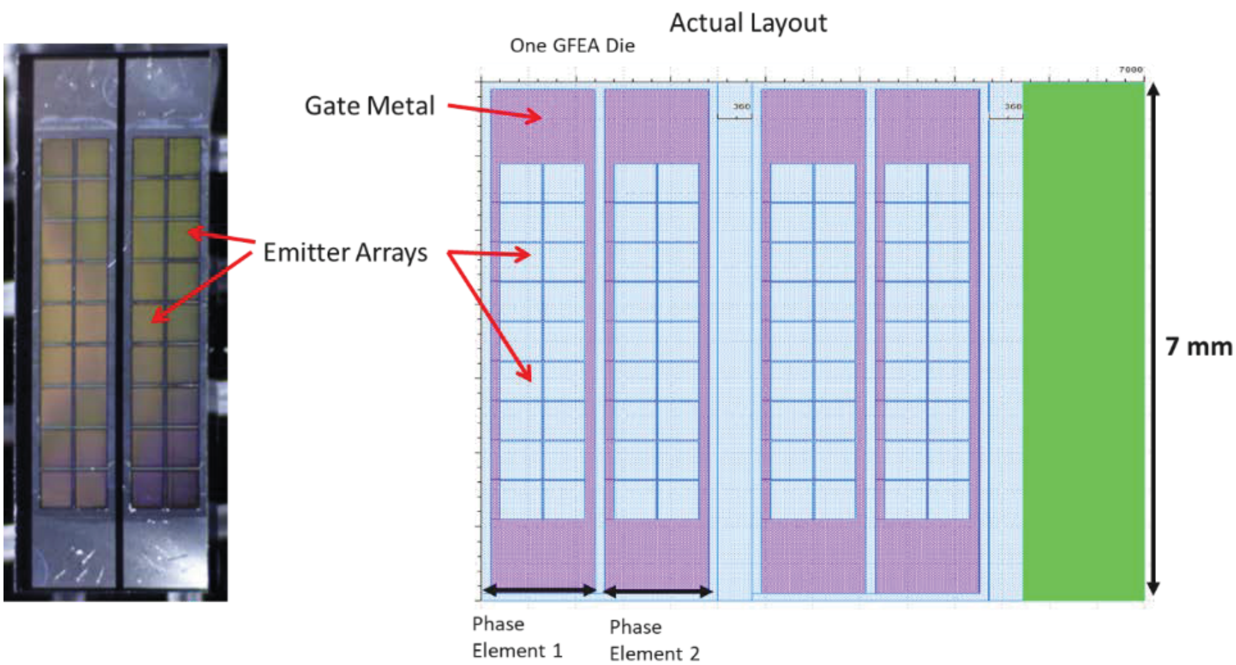

Figure 14. (Left) Microscopes image of a fabricated GFEA die .(Right)GFEA layout drawing shows 2 die plus a test section with each die divided into 2 phase element sections. Each GFEA die is also divided into subsections for uniformity.

In this drawing the single die is divided into 2 phase elements, and the active area is divided into a grid pattern for the gate metal to ensure minimal voltage drop. This technique was used in Field Emission Displays to improve uniformity, and it was found to be very effective. The GFEA fabrication process is designed to create very high performance emitters with high current density (~100 A/cm^2) and low gate voltage (~70 V). For our experiments, bases on the die design, we will need ~200 mA/cm^2. Therefore, the devices are operating roughly 500 times below their maximum current density. This lower current density should greatly improve the yield of the die after fabrication and test. It also decreases the voltage driving requirements as explained above.

The actual emitter structures can be seen in Fig. 15 where a pictorial of the die concept is shown along with SEM images of actual die structures. We received these die from MIT and began extensive testing as described in the next section of this report. These die did not achieve the required current requirements and suffered from high leakage because of fabrication issues. However, more recent tests at MIT have shown both higher current over larger areas but also the capability of modulating the cathodes at higher frequencies although not the 1 GHz need for the magnetron. Extensive analysis at MIT has indicated some of the process problems including with the uniformity of the tip etch and with the CMP process. These processes must be fixed for successful fabrication of GFEAs needed for this project.

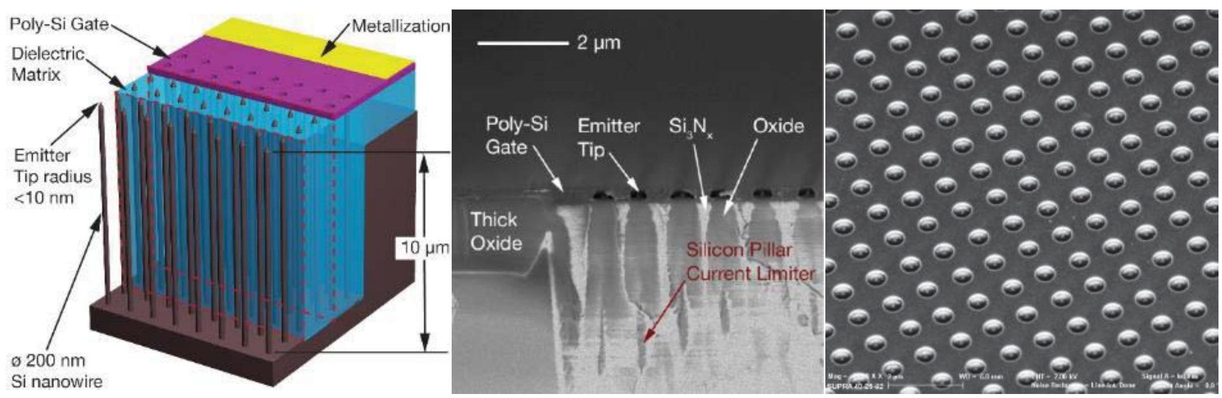

Figure 15: *Silicon Field Emitter Array Cathode based on a 2D array of self-aligned gated Field Emitters individually regulated by silicon nanowire current limiters. On the left handside is a schematic diagram of our device, in the middle is a SEM cross-section showing the tips on top of silicon nanowires within a gate aperture (≈350 nm) and on the right hand side is SEM of the top view of the device showing that tips are arranged in a 1 μm square grid leading to a tip density of 10^8 tips/cm^2. Each tip is capable of emitting 1 μA.*

D. MIT test results

The GFEA die at MIT are tested in the system shown in Fig. 16. This particular image shows the pulsed driving system for testing the emitters at frequency. This system was used extensively to determine the IV characteristics of probed GFEAs. Figure 17 shows a photograph of the inside of the chamber system with wafer section visible and the probe arms. Results from such tests are also shown in Fig. 18. Here a 20 A/cm^2 current density pulse is achieved with a 20 μs pulse width. These results clearly show the needed current density although not at the required frequency (1 GHz) which is not possible with the MIT system. Nevertheless, the required current density was achieved in those test structures.

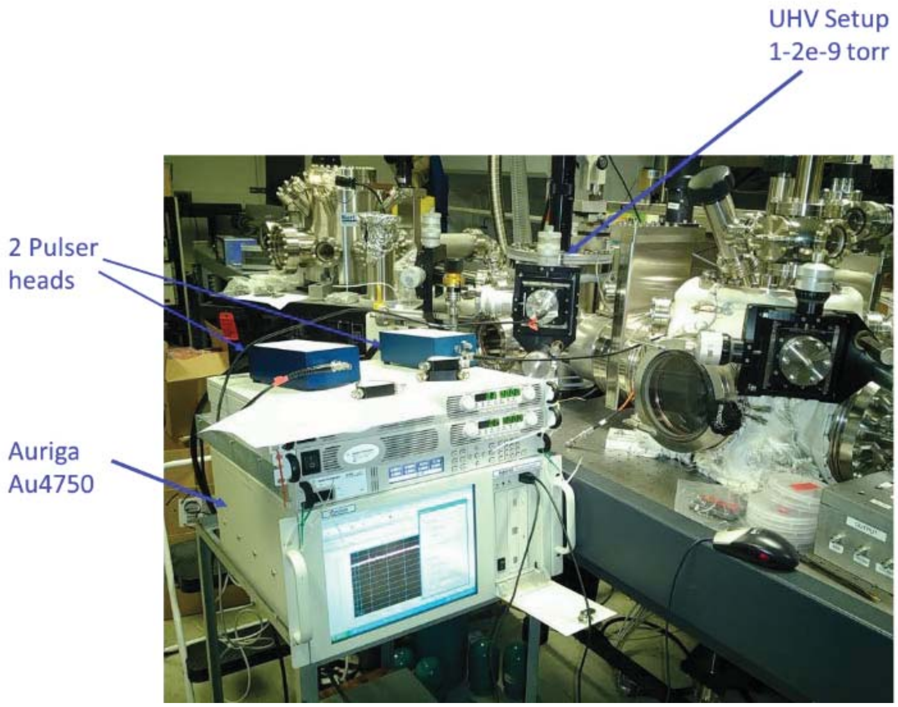

Figure 16. Photograph of MIT GFEA test system with pulse driver supplies.

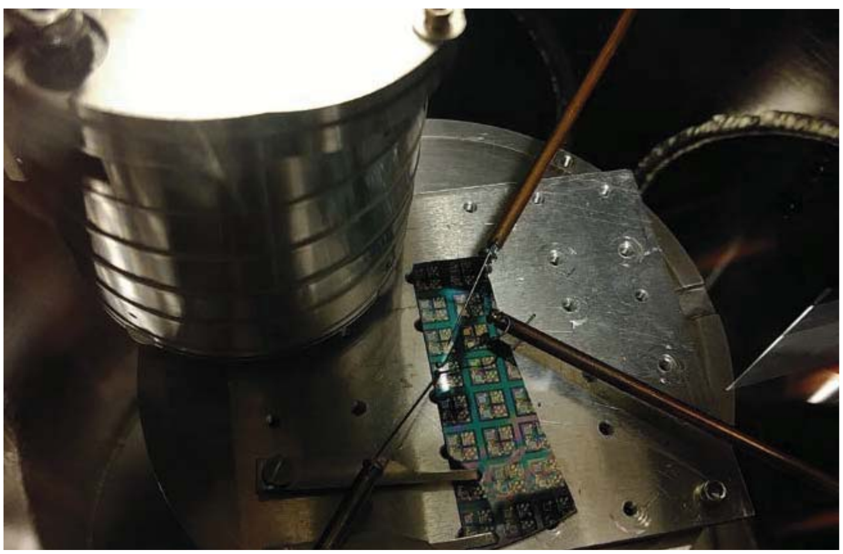

Figure 17. Photograph of the vacuum test chamber probe configuration.

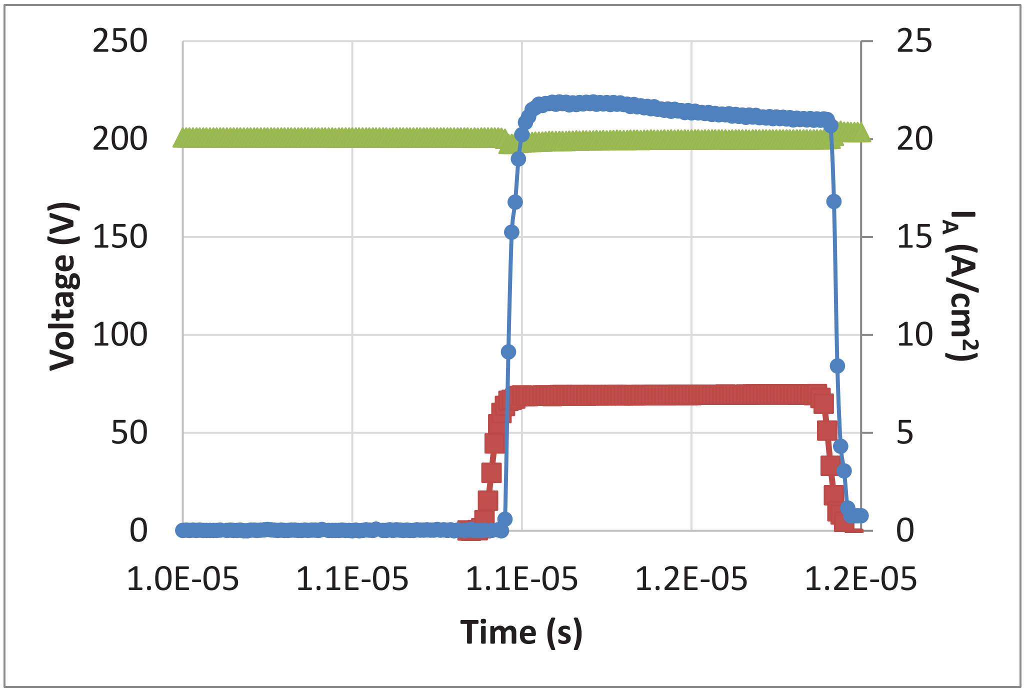

Figure 18. Pulsed IV curve of MIT GFEA showing a 20 A/cm^2 current density in a 20 us pulse.

VII. GFEA Die Testing at BSU

MIT shipped sections of wafers to BSU for GFEA testing. The wafers were first coated with photoresist to protect the emitters from particle shorts and then sawed. Shown in Fig. 19 is a photograph of a wafer section after delivery at BSU. A pick&place process was developed in which GFEA die were removed the saw backing tape and placed in an acetone bath as shown in the right side of the image. After the bulk of the resist is removed, the die are moved to a "clean" acetone bath followed by a DI water bath. Cleaned die are placed on a cloth to dry. Next, a wand is used to pick up the die at the interconnect pad section, and silver paste is painted on the back of the die for back-side ground connection to the silicon, which is the emitter tip. After drying, the die are stored in a die gel-pack.

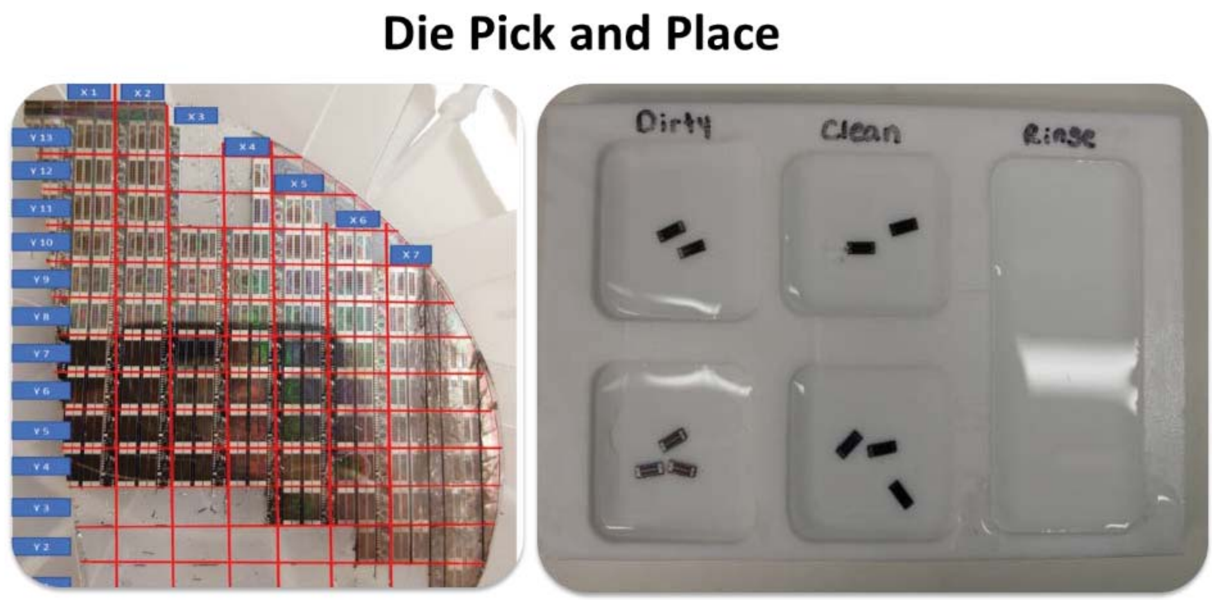

Figure 19. Photographs of (left) GFEA wafer section from MIT coated with resist and sawed into individual die and (right) photograph of the die strip containers where acetone is used in clean and dirty trays followed by a DI rinse.

Following die pick, the die are readied for testing using an LTCC based test structure. This structure is shown in a photograph in Fig. 20. As seen the structure holds 8 GFEA die for testing in vacuum. Each die is placed in a slot which has silver traces connected through vias to a shared ground plane. Silver tape is used to make a temporary connection from the back side of the die to the silver paste. Once the die is in place, silver tape is placed across the end connection pad as seen in the photograph. This connection is to the gate of the emitter structure array. This connection electrically address both phase elements of the GFEA die. Electrical connectivity is checked by using a meter to measure the resistance from the gate to the ground. This process has been found to be effective but non-trivial. It requires training to properly place the silver tape to prevent both opens and shorts. It can also result in damage to the die if not carefully performed.

Once the GFEA die are ready for test, they are placed in a vacuum chamber which is pumped with a turbo pump to 10^{-7} Torr. Electrical feeds allow connection to a driver system which can test one die at a time. A pulsing circuit provides a 0.1 – 1ms long pulse with a 10% duty cycle. The driver an go up to 80 V and also allows for a DC offset. A ZnO:Zn phosphor screen is placed over the array. Electron emission excites the screen which is biased at 1000 V. An excited screen is seen in Fig. 20 where the blue green light is observed. This image is of a GFEA die under test. Over 200 GFEA die were tested in this project with ~10% showing emission, but none achieved the required 5 mA of current needed for the project. The primary issues were gate-emitter leakage before testing and arcing during testing. Die that emitted current often arced (failed) when driven above 50 V. As part of the test procedure, leakage current before and after testing was measured along with anode current during emission. An example of the measured anode current of one die is shown in Fig. 21. **This GFEA die test procedure and system is complete, and more than 200 die have been tested.**

GFEA Die Test

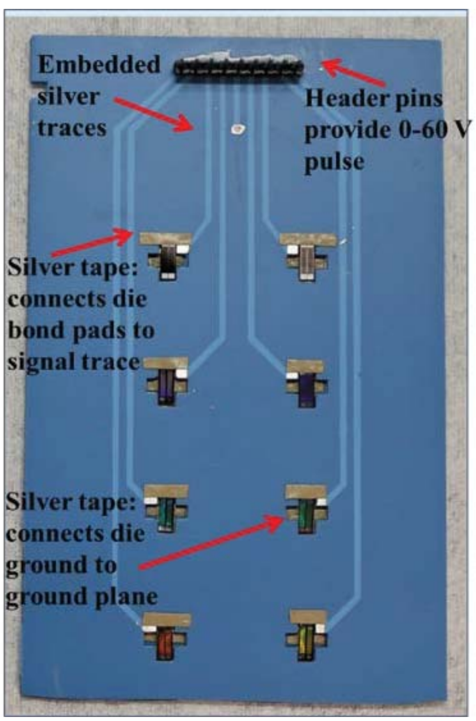

Vacuum Test with Phosphor

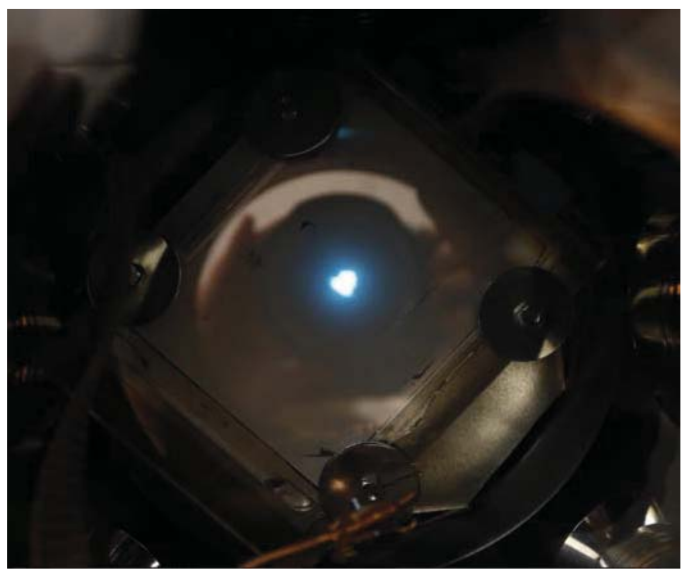

Figure 20. (Left) Photograph of the GFEA test structure for temporary electrical connections to the die for testing in vacuum and (right) photograph of the phosphor screen in the test chamber excited by a GFEA die.

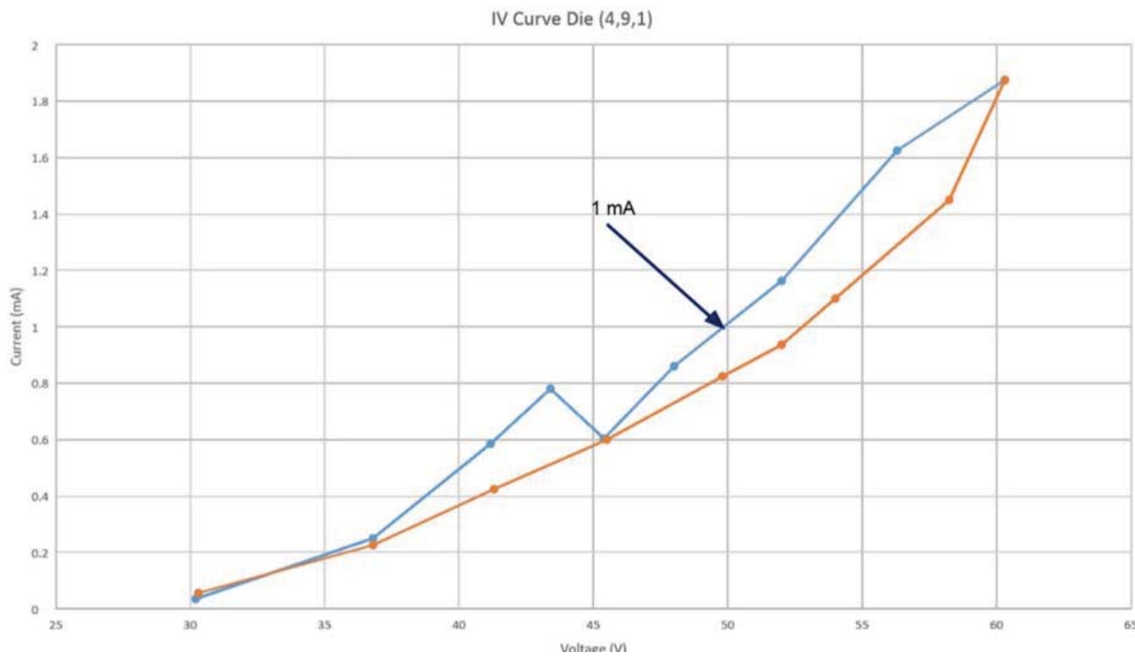

Figure 21. IV curve of a GFEA die as measured using a current transformer in the vacuum test chamber. The die achieved 1.8 mA before arcing at 60 V. The 2 traces are of the same die with different voltage sweeps.

VIII. Simulation of the L3 Magnetron with Cathode Modulation

A. Magnetron Model 1

Our original simulation efforts used a batch input method for the PIC code Vsim to create the magnetron model of the L3 industrial magnetron. A range of efforts to properly model the magnetron were attempted. After a range of studies, the model shown in Fig. 22 was developed and implemented. The model, however, did not have a pi-mode at 907 MHz as expected. Instead, the device operated at 923 MHz. Numerous studies went into to understanding these issues. However, the pi-mode discrepancy was not remedied until a Magnetron Model 2 was developed as described below. Despite this issue, extensive simulations were performed to look at magnetron oscillation and the use of a modulated cathode using this first model. The cross sectional view is shown in Fig. 23.

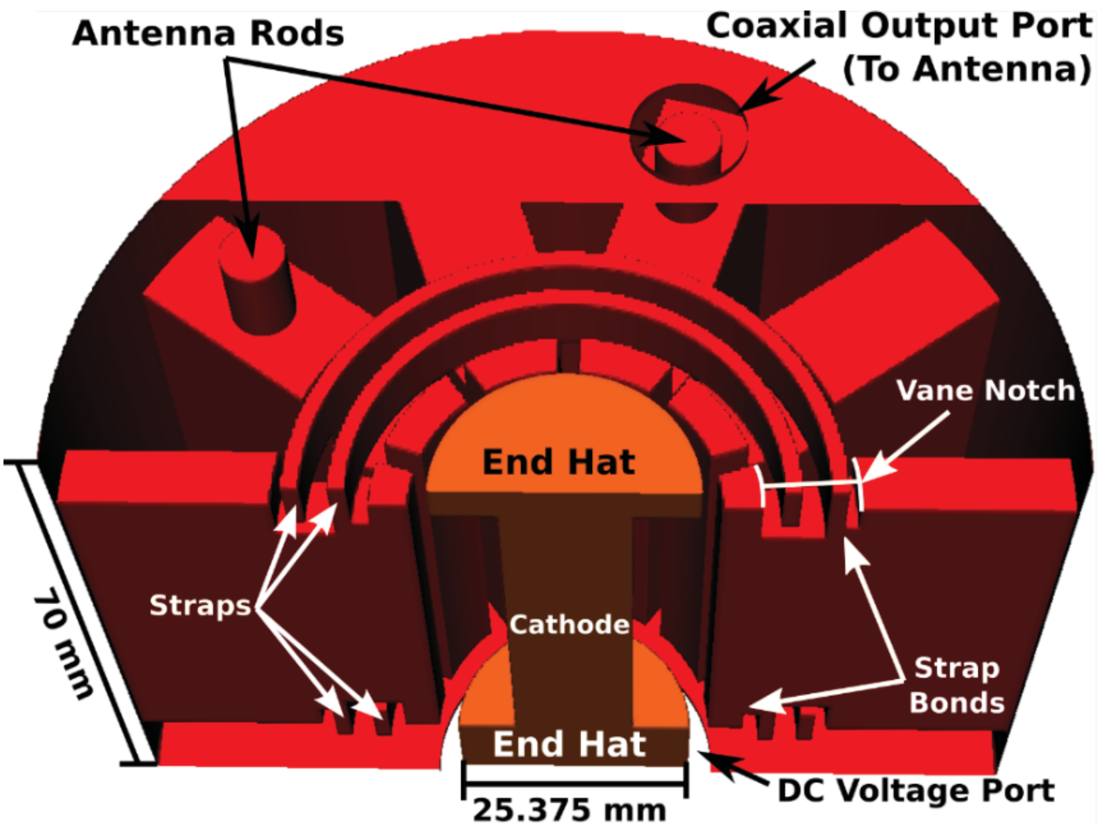

Figure 22. The Vsim model of the L3 industrial magnetron showing the simple cylindrical cathode, end hats, straps, and vanes. The model ends at the coaxial output ports (antennas) and does not extend to include the full antenna structure

In this model, a mesh of 261x261x84 was used to keep simulation times reasonable. The typical simulation parameters were -17 kV, 1700 G, and 5 A of injected current; however a number of other operating parameters were studied over the course of the project. It was discovered that is was not possible to start oscillation with this model without some form of "priming". When the

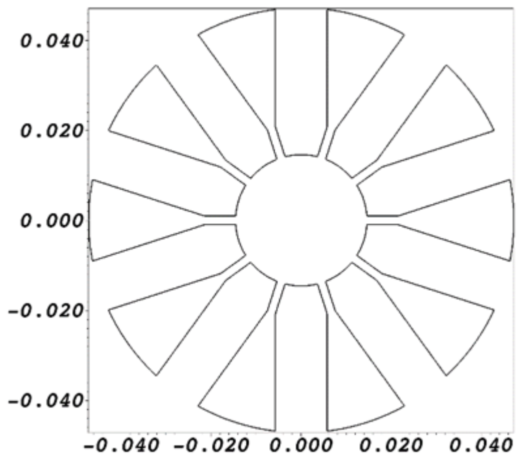

Figure 23. Cross-sectional view of the Vsaim magnetron model at the axial center of the structure. Not cathode is shown.

field are high (-17 kV, 1700 G), the electrons are trapped near the cathode, and little interaction is seen up to a simulation time of ~200 ns. Even at lower fields (-9kV, 800 G) where the electron hub is nearer the anode, it was difficult to get oscillations to start-up. Eventually, “RF priming” was used. In this method, a large RF signal is excited in the cavities of the magnetron at the oscillation frequency. In the most successful simulations, the RF priming was used for 20 ns and then turned off. Eventually oscillation would start. This result can be seen in Figures 24 and 25. Figure 24 shows the electrons in the simulation at 50 ns (no oscillation) and 100 ns (clear oscillation. This oscillation occurs ONLY because of RF priming. If not priming is used, the magnetron will not oscillate. Note that studies of shorter RF priming time times have not been performed. The cavity oscillation is shown in Figure 25, This figure shows the very large RF priming signal at the start which is then stopped. The oscillation then takes 75 ns to fully start-up. **This result represents the first demonstration of simulation oscillation of the L3 industrial cooker magnetron.**

Despite these results, there were several issues. Cathode modulation runs showed a variety of start-up issues and inconsistencies. In particular, it was noticed that the antenna ports were out-of-phase. As seen in Figure 26, the voltages on the three antenna ports are plotted on the top with the cavity voltage on the bottom. In the actual magnetron the three ports extend to an antenn and are connected electrically by that antenna. Hence, the voltage on the 3 ports should be nearly identical and in-phase. However, the ports are not only out-of-phase

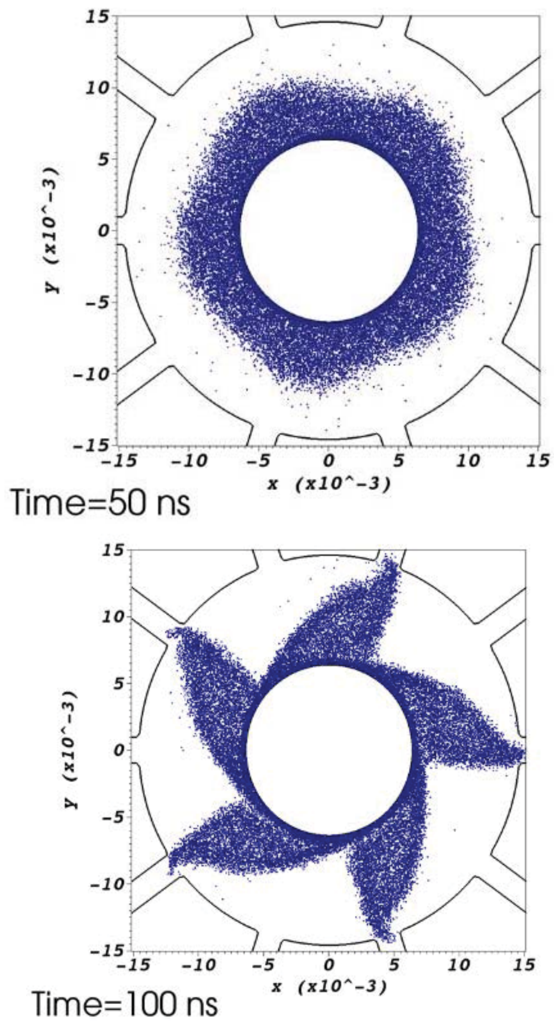

Figure 24. Simulation of the magnetron using RF priming at 50 ns (top) and 100 ns (bottom) where oscillation occurs because of the priming.

but also drifting with respect to the cavity voltage. This variation eventually led to the decision to create a new model which included the full antenna structure: Magnetron Model 2.

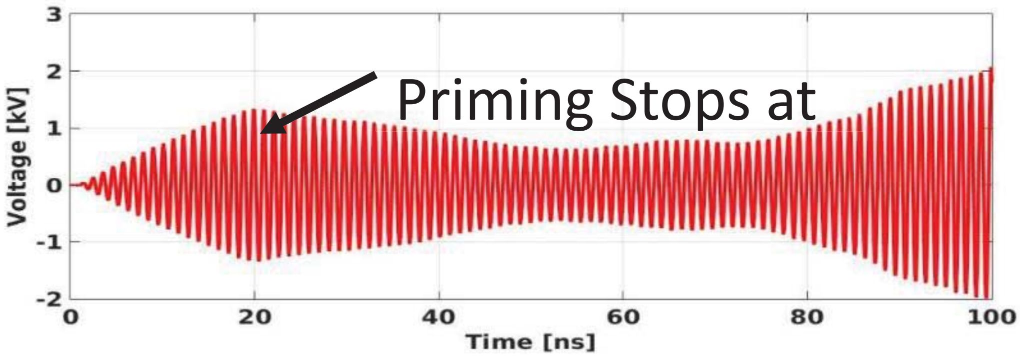

Figure 25. RF cavity voltage in Vsim using RF priming for 20 ns after which it is turned off. The simulation thes shows oscillation start at 100 ns.

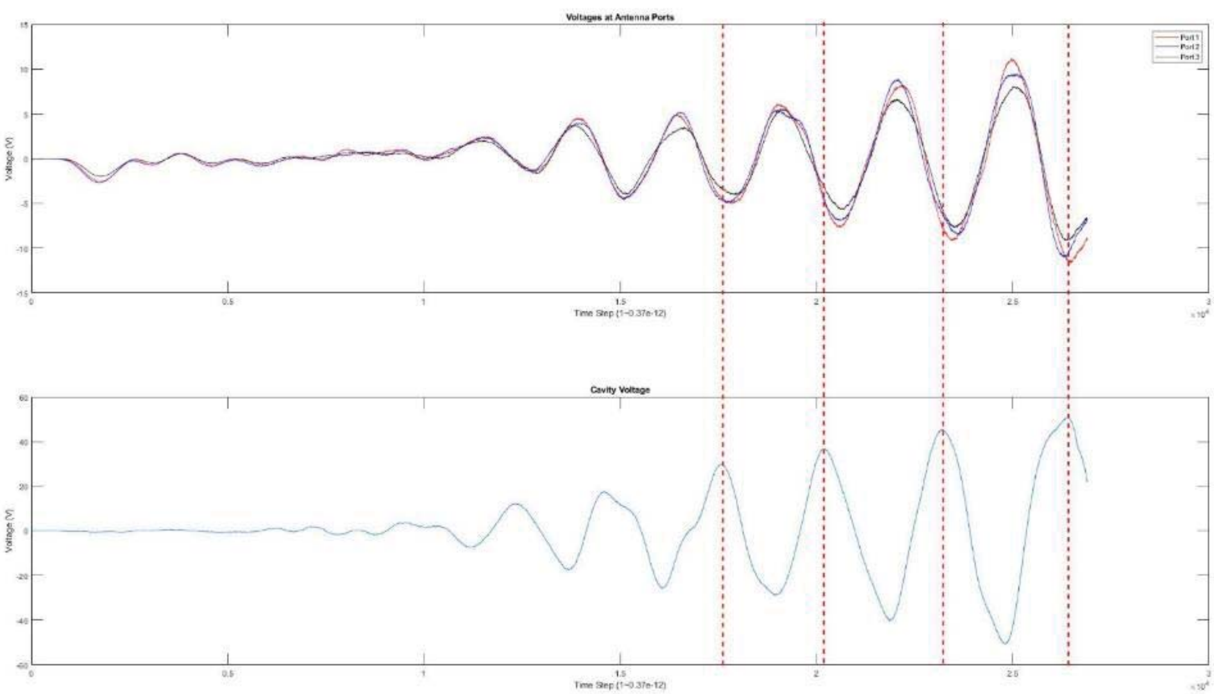

Figure 26. The antenna ports (top) and the cavity voltage (bottom) during a simulation. Note that the signals are out-of-phase even though the ports should be at the same phase. Also note that the cavity voltage varies in phase relative to these ports.

B. Magnetron Model 2

Based on the issues with the pi-mode frequency and the phase variation at the 3 output ports, the VSim model underwent a complete rework using the newly developed VSim GUI. The previous VSim model used hard-coded functions to construct the magnetron geometry, and the magnetron geometry did not include the structure which tied the three antenna rods together. The reworked model imports STL files to construct the magnetron geometry in the simulation. These STL files were constructed in Google SketchUp based on the physical parameters of the L3 CWM-75kW magnetron. The reworked model includes the complete antenna geometry which connects the three antenna rods to one single output antenna as shown in Fig. 27. Consequently, RF power generated by the resonance circuit now exits the simulation domain at a single location instead of at three separate locations as in the previous model.

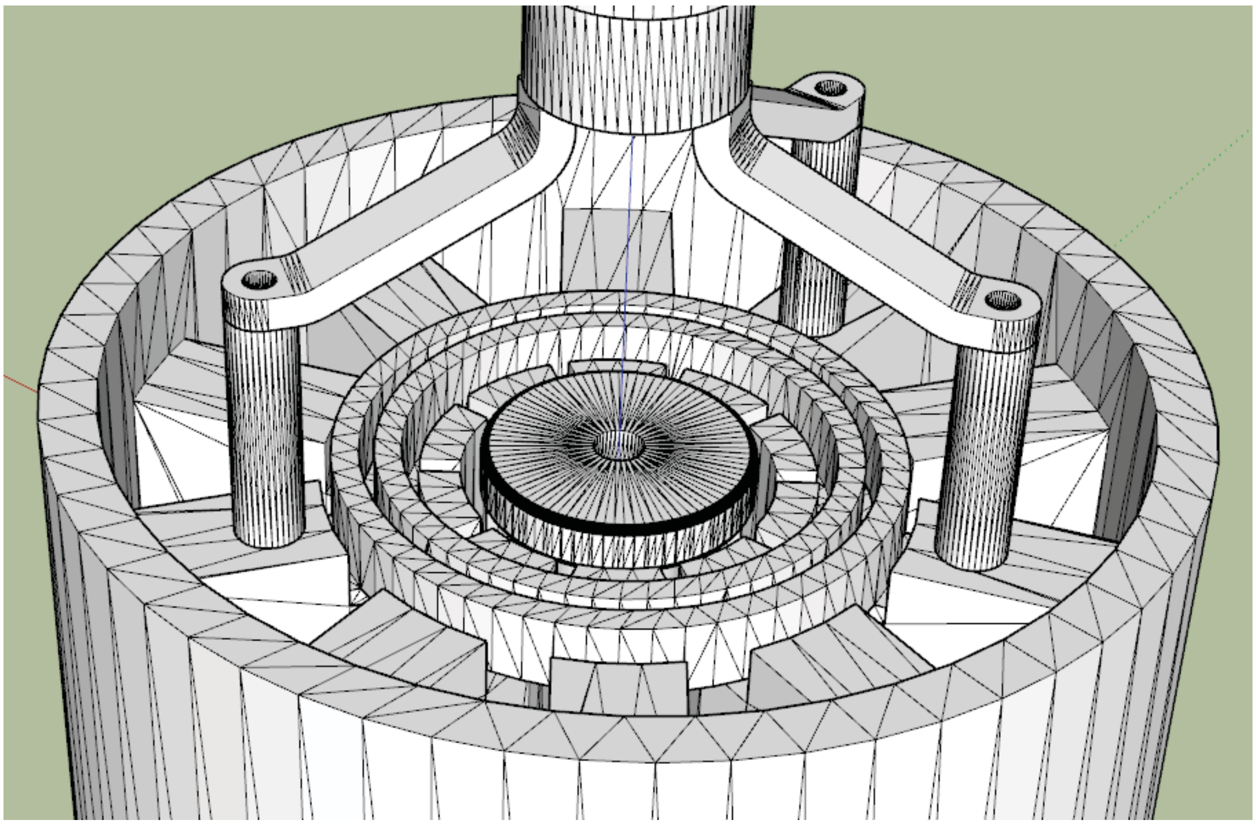

Figure 27. CAD Drawing of the Reworked Geometry Featuring the Complete Antenna Structure

The reworked model also can include a 10-side-faceted cathode geometry in replacement of the cylindrical cathode in the previous model. This new cathode, shown in Figure 28, represents the 10-sideds faceted cathode used in the experiment.

Figure 28. 10-Side-Faceted Cathode as Seen in the VSim GUI. The top and bottom are the end-hat structures.

The DC voltage between the anode and the cathode in the reworked model was generated by defining a D-field between the anode geometry and the cathode geometry at the bottom of the simulation domain (lower Z). The static magnetic field was defined as a uniform external field in the -z direction over the entire simulation domain. Finally, electrons were emitted from the flat sections of the cathode surface via the Richardson-Dushman emission profile available in VSim. Each modulated section represents ½ of the cathode facet surface to approximate the experiment. As with Model 1, the cathode can be modulated to create the electron injection for the spokes at the desired frequency. Shown in Fig. 29 are the simulations for different times using the modulated electrons. The latest simulations used the following list of parameters (Table 2):

Table 2. Simulation parameters with cathode modulation

Anode-Cathode DC Voltage	~17kV
Static Magnetic Field Strength	1700G
Cathode Emission Current	~5A
Cathode Modulation Frequency	915MHz
RF Priming	None

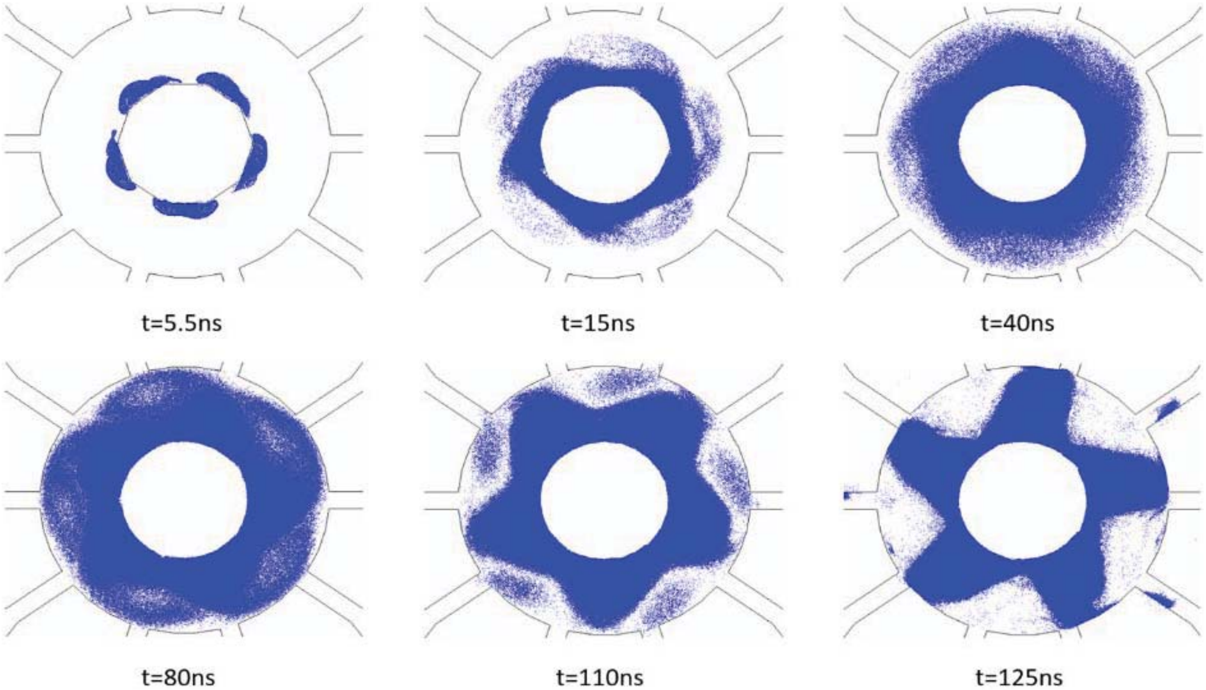

Figure 29. Temporal evolution of electron spokes in Vsim using cathode modulation. The first capture (5.5 ns) shows that electrons are injected only where needed in order to form the spokes. The magnetron is in oscillation ~125 ns.

The cavity voltage plot is shown in Figure 30. The growing oscillation voltage is clear with full oscillation ~125 ns.

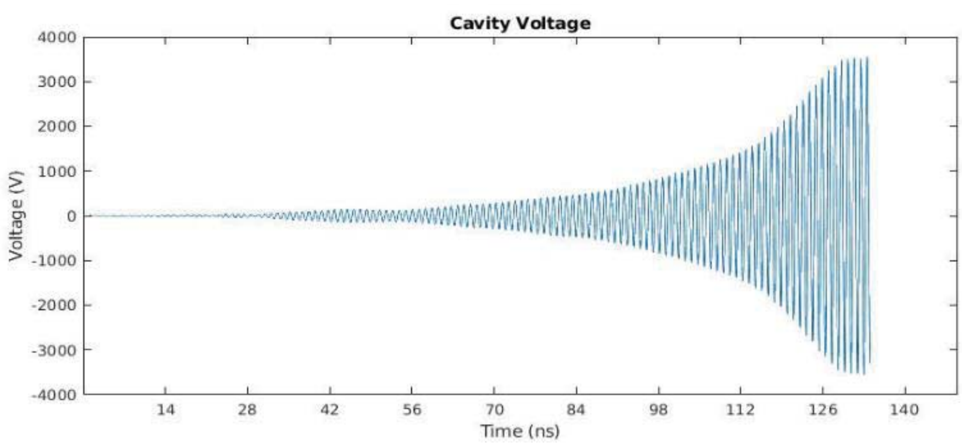

Figure 30. Cavity Voltage Plot showing eventual oscillation at 130 ns from the use of cathode modulation.

Figure 31 shows the over plots of RF periods after the model reached full oscillation, and Figure 32 shows a zoomed-in version near the tail end of RF periods. According to the specification sheet of the L3 CWM-75kW, the magnetron has operating modes at 896MHz, 915MHz, 922MHz, and 929MHz. The plots above show that the oscillation frequency is “hopping” between the 896MHz mode and the 915MHz mode. The modulated cathode should be driving the oscillation at the 915 MHz mode, but this is not occurring. Careful study of the electron injection and the electron spokes during oscillation show that the injected electrons become out-of-phase with the spokes. The cause of this desynchronization between phase of cathode modulation and the phase of the electron spokes is under study and may be related to a variation in the cathode voltage in the model. A more detailed study of the simulation model and the magnetron device physics is required. **However, the results clearly show that the cathode modulation can be used to start up oscillation in this industrial magnetron.**

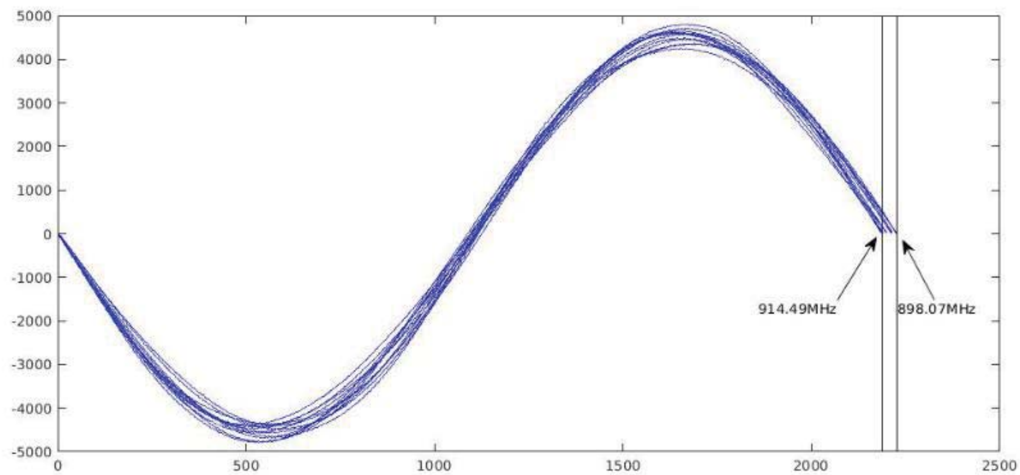

Figure 31. Over Plots of RF Periods After the Model Reached Full Oscillation

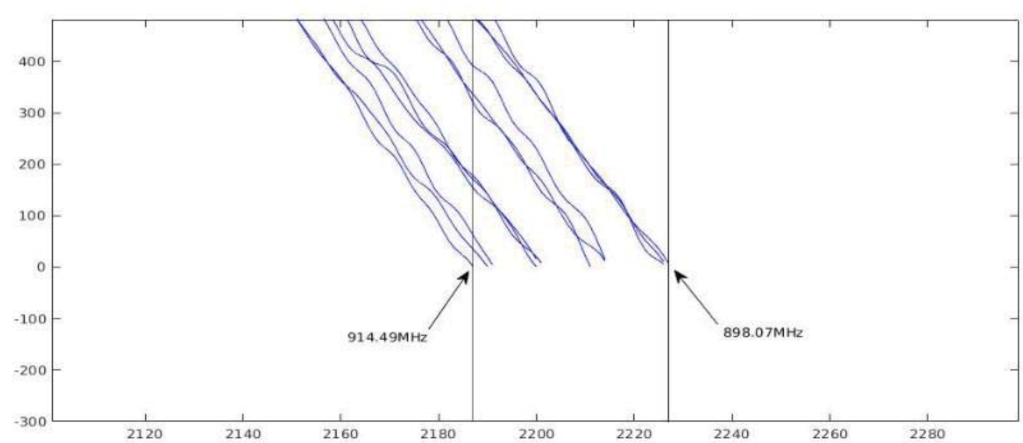

Figure 32. Over Plots of RF Periods After the Model Reached Full Oscillation (Zoomed-In)

IX. Presentations and Students

A. Presentations

Andong Yue, Ryan Harper, Daylon Black, Don Plumlee, Tayo Akinwande, Winston Chern, Mike Worthington, John Cipolla, and Jim Browning, “An Industrial Magnetron Using Gated Field Emission Arrays for Phase-Control,” to be presented at the IEEE International Vacuum Nano-Electronics Conference, Cincinnati, OH, July (2019)

A.Yue, J. Browning, M. Worthington, J. Cipolla, “Simulation of an Industrial Magnetron Using Cathode Modulation, “ IEEE Conference on Plasma Science, Orlando, FL, June (2019).

Marcus Pearlman, Andy Yue, Jim Browning, Mike Worthington, and John Cipolla, “SIMULATION OF AN INDUSTRIAL MAGNETRON WITH PHASE CONTROL USING A MODULATED CATHODE,” IEEE Inter. Conf. on Plasma Science, Denver, CO, June (2018)

R. Harper, M. Pearlman, A. Yue, S. Saldivar, T. Berntsen, T. Lu, S. Longmuir, O. Betnacourt, T. Moodley, P. Ward, D. Black, D. Plumlee, T. Wakinwande, W. Chern, and J. Browning, “DESIGN OF PHASE CONTROLLED MAGNETRON USING GATED FIELD EMISSION ARRAYS,” IEEE Inter. Conf. on Plasma Science, Denver, CO, June (2018).

J. Browning, M. Pearlman, D. Plumlee, T. Akinwande, M. Worhtington, and J. Cipolla, “DEVELOPMENT OF A PHASE-CONTROLLED MAGNETRON EXPERIMENT USING A MODULATED ELECTRON SOURCE,” IEEE Inter. Conference on Plasma Science, Atlantic City, NJ, June (2017).

J. Browning, V. Saxena, S. Plumlee, T. Akinwande, M. Worthington, and B. Hay, “A Phase-Controlled Magnetron Using a Modulated Electron Source,” IEEE Inter. Conf. on Plasma Science, Banff, Canada, June (2016). **DOI:** 10.1109/PLASMA.2016.7533988

J. Browning, M. Pearlman, D. Plumlee, T. Akinwande, M. Worthington, and J. Cipolla, “A phase-controlled magnetron using a modulated electron source,” Presented at the AFRL, Kirtland AFB, Albuquerque, NM, Dec. 12 (2016).

B. Thesis

Daylon Black, “NOVEL LOW TEMPERATURE COFIRED CERAMIC MANUFACTURING TECHNIQUES FOR A MAGNETRON FIELD EMISSION CATHODE” Master of Science Thesis in Mechanical Engineering (2019).

C. Students

BSU:

This project has included 16 undergraduate research students over three year program. Originally, a post-doctoral student was planned in year 1; however the student was delayed in graduation, and that student, Marcus Pearlman, worked on the project until July 2018. Two of the undergraduate students, Jacob Davlin and Omar Betancourt, were also a summer interns at L-3 Technologies, EDD in Williamsport, PA. Both JacoDavlin and another student researcher, Jenn Finbeiner, currently work for L3 Technologies. The students are:

Marcus Pearlman, Post-doctoral in ECE (1/3/17)
Andy Yue, ECE PhD student
Ryan Harper, ECE MS student
Daylon Black, MBE MS student (graduated)

Undergrad Students:
Jenn Finbeiner, MBE
Steven Saldivar, ECE
Tanaya Lu, ECE
Sean Weech, ECE
Jacob Davlin, MBE
Zach Taylor, MBE
Shayne Hansen, MBE
Andee Morton, MBE
Matt Beman, ECE
Antonio Marquez, MBE
Tiffany Berntsen, ECE
Tanya Lu, ECE
Patrick Ward, MBE
Patrick Epperson, ECE
David Vogel, ECE

X. Summary and Conclusions

The purpose of this project was to study the effects of a modulated cathode on an industrial magnetron in which the electrons were injected with both temporal and spatial control. The research included both experimental and simulation efforts. The experiment was based on the L3 Technologies CWM75KW industrial cooker magnetron which operates at a peak power of 75 kW from 900-915 MHz. For our experiment, a version of the device was provided by L3 Technologies without the cathode so that it could be mounted on a test chamber and operated at low power (~1 kW) using low current (~150 mA). A new cold cathode structure was developed using Gated Field Emission Arrays (GFEAs) as the electron source. The design allowed placement of 30 GFEA die in a cylindrical geometry with 3 die spaced axially and 10 die spaced azimuthally. Each die in the design is divided into 2 phase elements. These GFEA are to be driven by a “barber pole” delay transmission line so that 4 phase control elements can be used to drive 5 electron spokes at the desired frequency.

The cathode structure, delay line, and facet plates which cover the GFEA along with the appropriate electrical connections were designed and fabricated. GFEA die were attached to the structure and placed in the vacuum test chamber to demonstrate the process. The GFEA die, which must each generate 5-7 mA, were designed to match the cathode structure. The die were fabricated at MIT using their field emitter fabrication process. MIT delivered several hundred such die with over 150 tested in our test system. An entire die saw and test process was developed and successfully implemented. However, none of these die were able to achieve 5 mA without arcing or high leakage. Recent field emission structures tested at MIT have demonstrated a higher level of current capability in pulsed operation (10 μs pulse width). It is expected that a new generation of GFEA cathodes with improved process uniformity should meet our requirements.

Simulation of the magnetron has been performed using the PIC code Vsim. This extensive modeling effort went through 2 phases. In the first model, the magnetron was modeled with a cylindrical cathode and with 3 antenna ports rather than the complete antennas structure in order to reduce computation time. After a detailed analysis of results, it was believed that the lack of the tur antenna was creating loading problems on the magnetron and changing the operating frequency. A brand new model was created, and this model included the full antenna structure. This model has been tested under a number of conditions. With no external stimulation, the model will not oscillate when operated for 200 ns. However, if RF priming is used for as little as 20 ns, the device will oscillate in the simulation. In a second set of simulations, the model used a 10-sided cathode and electron modulation in order to approximate the planned cathode structure of the experiment. Electrons were injected to form the electron spokes at the oscillation frequency. This technique also shows start-up and oscillation. However, the results have not shown phase control.

REFERENCES

[1] Daylon Black, “NOVEL LOW TEMPERATURE COFIRED CERAMIC MANUFACTURING TECHNIQUES FOR A MAGNETRON FIELD EMISSION CATHODE” Master of Science Thesis in Mechanical Engineering (2019).

AFOSR Deliverables Submission Survey

Response ID:11287 Data

1.

Report Type

Final Report

Primary Contact Email
Contact email if there is a problem with the report.

JimBrowning@BoiseState.edu

Primary Contact Phone Number
Contact phone number if there is a problem with the report

2084262347

Organization / Institution name

Boise State University

Grant/Contract Title
The full title of the funded effort.

Phase-Controlled Magnetron Development

Grant/Contract Number
AFOSR assigned control number. It must begin with "FA9550" or "F49620" or "FA2386".

FA#9550-16-1-0083

Principal Investigator Name
The full name of the principal investigator on the grant or contract.

Jim Browning

Program Officer
The AFOSR Program Officer currently assigned to the award

Jason Marshall

Reporting Period Start Date

02/15/2016

Reporting Period End Date

02/14/2019

Abstract

This project involved the development of a cathode structure using Gated Field Emission Arrays (GFEAs) that could be modulated at the operating frequency of a magnetron to control electron injection. The goal was to inject the electrons to preferentially form the electron spokes in a 75 kW industrial cooker magnetron. An experiment was developed using the L3 Technologies CWM75KW which can operate as low as 1 kW with an injection current of 150 mA and at a frequency of 915 MHz. The experiment replaced the helical cathode in the magnetron with a ceramic based structure that used integrated interconnects, vias, and traces to support 30 GFEA die in a 10-sided configuration. Facet plates are placed over the die to protect them from the interaction space, and each plate had 2 slits which act as electron hop funnels. The entire cathode structure and GFEA test and integration process was completed. GFEA die were specifically designed for implementation into

the cathode structure. Each GFEA die was required to generate 5-7 mA to drive the magnetron; however only 2 mA was achieved for these large die because of shorting and leakage currents. Simulation efforts included a model of the magnetron using both a simple cylindrical cathode and a 10-sided cathode to match the experiment. Simulations at the typical magnetron parameters (5 A, -17 kV, and 1800 G) only demonstrated oscillation if cavity RF priming was used for as little as 20 ns with oscillation beginning at 100 ns. The modulated cathode concept was also studied with electron injection at the operating frequency to control spoke formation, and that model also showed oscillation after 120 ns.

Distribution Statement

This is block 12 on the SF298 form.

Distribution A - Approved for Public Release

Explanation for Distribution Statement

If this is not approved for public release, please provide a short explanation. E.g., contains proprietary information.

SF298 Form

Please attach your SF298 form. A blank SF298 can be found here. Please do not password protect or secure the PDF The maximum file size for an SF298 is 50MB.

SF_298_Browning_5_19.pdf

Upload the Report Document. File must be a PDF. Please do not password protect or secure the PDF . The maximum file size for the Report Document is 50MB.

FA9550-16-1-0083_BSU_Magnetron_Final_report_5_19.pdf

Upload a Report Document, if any. The maximum file size for the Report Document is 50MB.

Archival Publications (published) during reporting period:

New discoveries, inventions, or patent disclosures:

Do you have any discoveries, inventions, or patent disclosures to report for this period?

No

Please describe and include any notable dates

Do you plan to pursue a claim for personal or organizational intellectual property?

Changes in research objectives (if any):

Change in AFOSR Program Officer, if any:

Extensions granted or milestones slipped, if any:

Demonstration of gated field emission cathodes with necessary current was not achieved.

Demonstration of magnetron oscillation with cathodes was not achieved.

AFOSR LRIR Number

LRIR Title

Reporting Period

Laboratory Task Manager

Program Officer

Research Objectives

Technical Summary

Funding Summary by Cost Category (by FY, $K)

	Starting FY	FY+1	FY+2
Salary			
Equipment/Facilities			
Supplies			
Total			

Report Document

Report Document - Text Analysis

Report Document - Text Analysis

Appendix Documents

2. Thank You

E-mail user

May 15, 2019 13:18:26 Success: Email Sent to: JimBrowning@BoiseState.edu